Chapter

Rheology of Structured Oil Emulsion

Gudret Isfandiyar Kelbaliyev, Dilgam Babir Tagiyev and Manaf Rizvan Manafov

Abstract

This study is devoted to the rheology of oil emulsions, accompanied by both the formation and destruction of the structure. The presence of particles of a dispersed phase in an oil emulsion, including asphaltenes and resins, determines the formation of coagulation structures as a result of interaction and collision of particles. In this regard, to study the formation of coagulation structures, analytical solutions to the mass transfer equations are proposed, based on which the coalescence and fragmentation frequencies of the droplets are determined. Models and analytical solutions of the equation for the thinning of an interfacial film between droplets with their coalescence in the volume of an oil emulsion are proposed taking into account the Marangoni effect and the effect of asphaltene content. The thickness of the adsorbed layer on the droplet surface was estimated. Many empirical and semi-empirical formulas have been proposed for determining the dependence of viscosity on the content of water and asphalt-resinous substances in oil. Based on the solution of the Fokker-Planck equation, the evolution of the distribution function of droplets in time and size in an oil emulsion is studied.

Keywords: oil emulsion, rheology, coalescence, deformation, breaking, asphaltenes, drop, viscosity, Marangoni effect, distribution function

1. Introduction

The separation processes of oil emulsions are an important stage for the preparation and purification of crude oil from water, mineral salts and various related impurities, asphalt-resinous substances, and paraffins contained in oil. The processes of separation of oil emulsions, the purpose of which is to completely reduce their aggregative and kinetic stability, are carried out in various ways: in gravitational (settling systems and other modifications); in centrifugal, electric, and magnetic fields [1–4]; as well as using filtering through solid and liquid layers, using microwave and membrane technology [5, 6].

Oil emulsions contain water droplets of a sufficiently large size, in connection with which, in most practical applications, high-capacity separation processes use settling systems, and at small sizes and droplet concentrations, using a constant electric field and membrane technologies or combined methods to achieve high degree of purification.

Experimental and theoretical studies indicate a very complex, in disperse composition (separation) and in the flowing physical phenomena (coalescence,

deformation, crushing), the structure of the intermediate layer. Many works have been devoted to theoretical and experimental studies of the mechanism of the formation of stabilization and destruction of oil emulsions as heterogeneous media [2, 4]; although many problems associated with the phenomena occur at the oil–water interface, the coalescence and fragmentation of water droplets, separation, and deposition have not been resolved correctly. Oil emulsions are polydisperse media with droplet sizes of 1–150 microns, although coarse (150–1000 microns) and colloidal (0.001–1 microns) particles are found in them. Such a size dispersion has a significant effect on the mechanism of structure formation, structural destruction, separation, and precipitation of droplets in oil emulsions. The mechanism of destruction and coalescence of droplets in oil emulsions can be divided into the following stages [7, 8]:

a. Convergence and collision of droplets of different sizes with the formation of an interfacial film. It should be noted that droplet transfer in a polydisperse medium is determined mainly by hydrodynamic conditions and flow turbulence. Under conditions of isotropic turbulence, the collision frequency of droplets depends on the specific dissipation of the energy of the turbulent flow and the properties of the medium and the dispersed phase [9–12]. As a result of the collision and fixation of two drops with sizes a_1 and a_2, an interfacial film of circular cross section is formed, the radius of which can be determined in the form [13]

$$R_K = \left[\frac{3\pi}{4} P_m (k_1 + k_2) a_r\right]^{1/3} \tag{1}$$

where P_m is the maximum compressive pressure, k_1, k_2 are the elastic coefficients of two drops, $a_r = {}^{a_1 a_2}/_{(a_1+a_2)}$ is the average size of the drops, and a_1, a_2 are the diameters of two drops. In [14], the expression for the hydrodynamic compression pressure in a turbulent flow is defined as

$$P_m = \pi a_r^2 \rho_C \vec{U}^2 \tag{2}$$

b. The deformation and destruction of adsorption shells at the oil–water interface in the flow volume at certain temperatures ($60–70^0 C$) and pressures.

c. Thinning and rupture of the interfacial film, followed by coalescence and coarsening of the droplets. The rupture of the interfacial film contributes to the coalescence of smaller droplets into larger ones. It is important to note that as a result of the transport of the oil emulsion in the pipes, the droplet crushing rate is much higher than the coalescence rate, as a result of which the oil emulsion is characterized by a large dispersion of droplet size and polydispersity of the medium.

d. Precipitation of droplets and separation of the dispersed phase as a continuous phase (separation).

An equally important factor affecting the efficiency of separation of oil emulsions is the conditions of thinning, tearing of the interfacial film [7], and the coalescence rate associated with the destruction of the adsorbed film on the surface of the droplets with the participation of demulsifiers.

The rheology of oil emulsions is associated with the presence of coagulation phenomena of dispersed particles in the presence of asphalt-resinous substances, accompanied in most cases by structure formation. The rheological properties of oil emulsions largely depend on the state of aggregation (solid phase, droplets, gas bubbles) and the properties of the dispersion medium. However, the presence of a dispersed phase can significantly change these properties under the influence of adhesion forces between particles of a dispersed phase and their interaction with a dispersion medium. In free-dispersed systems, particles of a dispersed phase are not interconnected and are able to independently move in a dispersion medium. In connected dispersed systems, particles of the dispersed phase form continuous spatial networks (structures); they lose their ability to transitional movement, maintaining only oscillatory movements. Unstable disperse systems provide structure formation in the system, up to the formation of aggregates and a skeleton, which can negatively affect the structural state (viscosity, fluidity), changing rheological properties, as well as to obtain precipitation during phase separation, treatment of industrial emissions, wastewater, etc. Aggregate stability characterizes the ability of a dispersed system to maintain a uniform distribution of particles of a dispersed phase over the volume of a dispersed medium without their interaction, providing conditions for the stability of the medium to phase separation. The loss of aggregative stability in concentrated emulsions is associated with coagulation of particles and their enlargement and can manifest itself in the formation of a bulk structure in which the dispersion medium is evenly distributed, thereby changing the rheological properties of the medium. The aggregate stability of dispersed systems with respect to coagulation is determined by the coagulation rate, which, in addition to the intensity of Brownian and hydrodynamic motion and the number of collisions, depends on the properties of the surface layers surrounding the particles. A deeper coagulation process leads to the destruction of the interlayers of the medium and direct contact of the particles, resulting in the formation of rigid coagulation structures and aggregates of particles, or their complete merging in the case of a liquid and gaseous dispersed phase (coalescence) (**Figure 1**).

The formation of coagulation structures and aggregates in the flow volume significantly affects the physical properties of oil emulsions associated with a sharp increase in the structural viscosity of the medium.

Based on this, the aim of this work is to study (a) the phenomena of coalescence, deformation, and crushing of droplets in a turbulent flow and the formation of coagulation structures associated with this; (b) the effect of asphalt-resinous substances on the formation of adsorption films and the structural viscosity of emulsions; (c) issues related to thinning and tearing of an interfacial film; and (d) the evolution of the droplet size and time distribution functions, taking into account coalescence and fragmentation of the droplets.

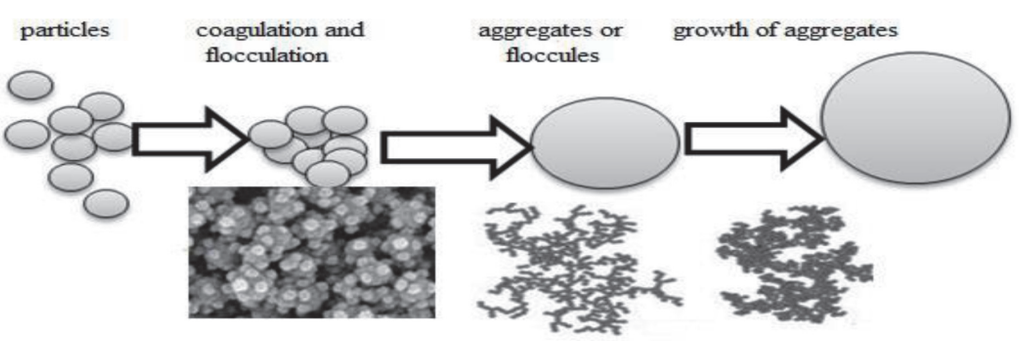

Figure 1.
Scheme of coagulation and formation of aggregates of particles of various structures.

2. Coalescence, deformation, and crushing of droplets in an oil emulsion

The structural and mechanical stability of emulsion systems is associated with the formation of adsorption layers at the oil–water interface, the composition of which consists of asphaltenes, resins, paraffins, mineral salts, and solid particles, i.e., natural surfactants [1–4]. It has been established that metal-paraffin complexes lead to the formation of the shell itself and solid particles (sand, clay, limestone, etc.) contribute to increasing the strength of the shells [3, 4]. An analysis of the composition of these shells on the surface of water droplets of crude oil of various fields shows that the main stabilizers are asphaltenes and resins, which include high-melting paraffins and inorganic mechanical impurities. The structure, composition, and physicochemical properties of asphaltenes, which are very complex compounds, are given in [14–17]. The formation of an adsorption layer on the surface of water droplets with elastic and viscous properties contributes to the stabilization of oil emulsions.

2.1 The influence of asphalt-resinous substances on the separation of oil emulsions

Consequently, the stability of oil emulsions is the result of a physical barrier that prevents tearing of the film when the collision energy between the droplets is insufficient to destroy the adsorption layer. The mechanism of the formation of adsorption films on the surface is determined by the following stages:

a. Diffusive mass transfer of the substance (asphaltenes) from the volume of oil to the surface of water droplets. In [18], the mass flow to the surface of a moving drop per unit time for small numbers $\mathrm{Re} = \frac{Ua_r}{\nu_c} << 1$ is defined as

$$I = \sqrt{\frac{\pi}{6}}\left[\frac{D}{a_r}\frac{\eta_C}{\eta_C + \eta_d}\right]^{1/2} a_r^2 \Delta C\sqrt{U} \tag{3}$$

where $\Delta C = C_0 - C_S$ and C_0, C_S are the contents of asphaltenes and resins in the volume and on the surface. Assuming that the change in the mass of the adsorbed layer is determined by $dm/d\tau = I$, integrating which we obtain $m - m_0 = I\tau$ (τ is the residence time, and m_0 is the initial mass of the adsorbed layer, taken equal to zero). Then, putting $m = \frac{1}{6}\pi\rho_a(a_r + 2\Delta)^3 - \frac{1}{6}\pi\rho_a a_r^3$ and taking into account the insignificance of the expansion terms of the second and third order of smallness ($\frac{\Delta}{a_r} << 1$), we have $m \approx \pi\rho_a a_r^3 \frac{\Delta}{a_r} = I\tau$. Taking into account expression (3), the thickness of the adsorbed layer is defined as

$$\frac{\Delta}{a_r} \approx \frac{1}{\sqrt{6\pi}}\left[\frac{1}{Pe}\frac{1}{1+\gamma}\right]^{1/2}\left(\frac{\Delta C}{\rho_a}St\right) \tag{4}$$

where $\gamma = \eta_d/\eta_C$, $\mathrm{Pe} = \frac{Ua_r}{D}$ is the Peclet number, $\mathrm{St} = \frac{U\tau}{a_r}$ is the modified Strouhal number, and ρ_a is the density of the adsorbed layer. It follows from Eq. (4) that the thickness of the adsorbed layer depends on the diffusion of particles to the surface of the droplet, the size and mobility of the surface of the droplets, and on the concentration of asphaltenes in the flow volume. For the values $Pe = 10^2 - 10^3$ ($D \approx 10^{-10} - 10^{-9}$ м^2/с), $\gamma = 0.8$, $\Delta C/\rho_a \approx 10^{-5}$, and $\mathrm{St} = 10^4 - 10^5$, from the equation, we estimate $\Delta/a_r \approx 0.01 - 0.03$. Large values of the number, which are the result of small values of the coefficient of diffusion of particles in a liquid, in some cases determine the prevalence of convective transport of

matter over diffusion. Further compaction of the adsorption layer under the influence of external perturbations and chemical transformations contribute to an increase in the density of the layer and the "aging" of emulsions. Despite the insignificant thickness of the adsorption layer compared to the size of the droplet, their strength on the surface of the droplets for various oils ranges from 0.5 to 1.1 $^{N}/_{m^2}$ [3].

b. Adsorption of the substance on the surface of the droplets.

c. Desorption and destruction of the adsorption layer with the participation of surface-active substances (surfactants). If the rate of adsorption and desorption is low compared to the rate of supply of the substance to the surface of the droplet, the process of formation of the adsorption layer is limited by the processes of adsorption and desorption. Assume that the concentration of adsorbed matter in the volume C_0 and on the surface Γ. By analogy with the derivation of the Langmuir equation, if we assume that the adsorption rate of the substance on the surface of the droplet is $W_A = \beta C_0\left(1 - {}^{\Gamma}/_{\Gamma_\infty}\right)$ and the desorption rate is $W_D = \alpha\Gamma$, then in the equilibrium state $(W_A = W_D)$, we have

$$\Gamma = \frac{KC_0}{1 + K_0 C_0} \tag{5}$$

where α, β are some constants, depending on temperature, $K = {}^{\beta}/_{\alpha}$, $K_0 = {}^{\beta}/_{\alpha\Gamma_\infty}$, and Γ_∞ is the maximum saturation of the droplet surface. Eq. (3) is in good agreement with many experimental data for oils of various fields. **Figure 2** shows the adsorption isotherm of asphaltenes on the surface of water droplets (T = 40°C) [19] for North Caucasian oils and the calculated values according to Eq. (5), where $K = 55, K_0 = 0.5$.

To destroy the adsorption films in the flow volume, various demulsifiers (SAS) are used, which are characterized by high surface activity during adsorption. The mechanism of destruction of adsorption films consists in the diffusion transfer of the demulsifier to the film surface, with further adsorption and penetration of the film into its volume, the formation of defects and cracks in its structure, a change in surface tension, and a decrease in strength properties, which qualitatively changes the rheological properties of the films at the oil-gas interface water. Further separation of oil emulsions is determined by the frequency of droplet collisions, their fixation on the surface, thinning, and rupture of the interfacial film.

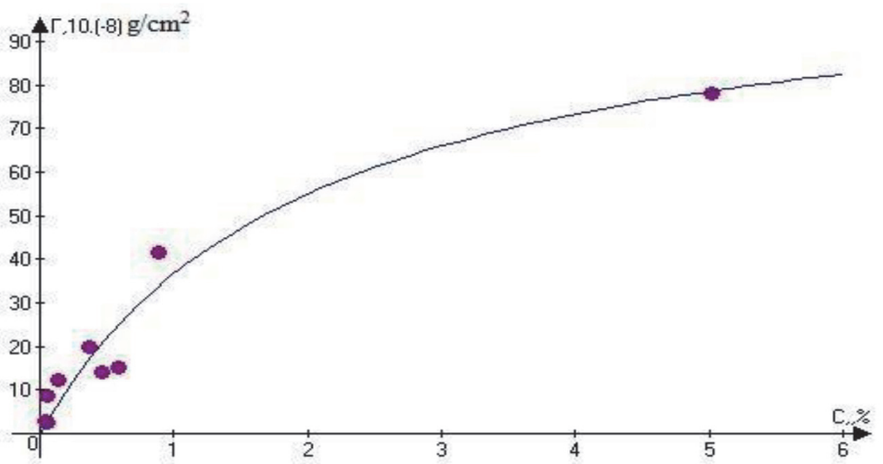

Figure 2.
Dependence of the concentration of adsorbed matter on the surface on the concentration of asphaltenes (points—experiment [19]).

2.2 Thinning and destruction of the interfacial film taking into account the Marangoni effect

When fixing two drops as a result of their collision, the resulting interfacial film under the action of various kinds of forces is thinned to a certain critical thickness and breaks with the further merging of two drops. Assuming that in a flat film of circular cross section the laminar flow, the momentum transfer equation in cylindrical coordinates is written in the form [7, 8].

$$-\frac{\partial P}{\partial r}+\frac{\eta}{gr^2}\frac{\partial^2 V_r}{\partial \theta^2}+\frac{\eta}{g}\frac{\partial^2 V_r}{\partial x^2}=0 \tag{6}$$

$$-\frac{1}{r}\frac{\partial P}{\partial \theta}+\frac{2\eta}{gr^2}\frac{\partial V_r}{\partial \theta}=0 \tag{7}$$

$$\frac{\partial V_x}{\partial x}+\frac{1}{r}\frac{\partial (rV_r)}{\partial r}=0 \tag{8}$$

where P is the pressure in the film, V_r, V_x are the components of the flow velocity in the film, and θ is the polar angle. The boundary conditions for solving these equations are

$$x=\delta,\ -\eta\frac{\partial V_r}{\partial r}=\frac{d\sigma}{dr}+\frac{1}{R_K\sin\theta}\frac{\partial \sigma(\cos\theta)}{\partial \theta} \tag{9}$$

The last condition determines the presence of convective flow in the film according to the Marangoni effect [20–22]. The Marangoni effect can be considered as a thermocapillary flow due to a change in the temperature in the film and a convective flow due to a change in the concentration of the demulsifier and surface tension. Then differentiating (7) with respect to θ

$$\frac{\partial^2 V_r}{\partial \theta^2}=\frac{r}{2\eta g}\frac{\partial^2 P}{\partial \theta^2}$$

and substituting into Eq. (6), we obtain

$$\frac{\eta}{g}\frac{\partial^2 V_r}{\partial x^2}=\frac{\partial P}{\partial r}-\frac{1}{2r}\frac{\partial^2 P}{\partial \theta^2} \tag{10}$$

Integrating Eq. (10) twice and using boundary conditions (9), we obtain

$$V_r=\frac{g}{\eta}\left(\frac{\partial P}{\partial r}-\frac{1}{2r}\frac{\partial^2 P}{\partial \theta^2}\right)\left(\frac{x^2}{2}-\delta x\right)-\frac{x}{\eta}\left(\frac{\partial \sigma}{\partial r}+\frac{1}{R_K\sin\theta}\frac{\partial \sigma(\cos\theta)}{\partial \theta}\right) \tag{11}$$

Solving Eq. (8), taking into account (11), and provided that the value is negligible, we obtain

$$V_x=\frac{d\delta}{dt}=-\frac{1}{r}\frac{\partial}{\partial r}\int_0^{\delta} rV_r dx=\frac{g\delta^3}{3\eta r}\frac{\partial}{\partial r}\left[r\left(\frac{\partial P}{\partial r}-\frac{1}{2r}\frac{\partial^2 P}{\partial \theta^2}\right)\right]+\frac{\delta^2}{2\eta r}\left(\frac{\partial \sigma}{\partial r}+\frac{1}{R_K\sin\theta}\frac{\partial \sigma(\cos\theta)}{\partial \theta}\right) \tag{12}$$

It should be noted that in [19] this equation was proposed in a slightly different form, not taking into account the distribution of pressure and surface tension depending on the angle θ. This wave equation determines the distribution of fluid velocity in the film or the change in film thickness depending on the pressure and distribution of surface tension. Neglecting the second derivatives $\partial^2 P/\partial\theta^2$ and $\partial^2\sigma/\partial r^2$, we obtain

$$\frac{1}{r}\frac{\partial}{\partial r}\left(r\frac{\partial P}{\partial r}\right) = \frac{3\eta}{g\delta^3}V_x - \frac{3}{2g\delta r}\left(\frac{\partial\sigma}{\partial r} + \frac{1}{R_K\sin\theta}\frac{\partial\sigma(\cos\theta)}{\partial\theta}\right) \tag{13}$$

Integrating Eq. (13) twice, provided that $r = R_K$ and $P = P_0(R_K)$, we obtain

$$\begin{aligned} P(r) = P_0(R_K) + \frac{3V_x\eta}{2\delta^3 g}\left(R_K^2 - r^2\right) - \\ \frac{3}{2g\delta}\left(\Delta\sigma(r)\ln\frac{r}{R_K} + \frac{r}{R_K\sin\theta}\frac{\partial\sigma(\cos\theta)}{\partial\theta}\right) \end{aligned} \tag{14}$$

where $P_0(R_K)$ is the external pressure at the periphery of the film. The force acting on the interfacial film with a uniform distribution of matter along the radius ($\Delta\sigma(r) \approx 0$) is

$$F = \int_0^{R_K} P(r)ds \approx P_0\pi R_K^2 + \frac{3\pi V_x}{2g}\frac{\eta R_K^4}{\delta^3} - \frac{\pi R_K^2}{g\delta\sin\theta}\frac{\partial\sigma}{\partial\theta} \tag{15}$$

Putting that $\Delta P = F - P_0\pi R_K^2$, we define

$$V_x = \frac{2g\delta^3}{3\pi\eta R_K^4}\Delta P + \frac{2\delta^2}{3\eta R_K^2\sin\theta}\frac{\partial\sigma}{\partial\theta} \tag{16}$$

Putting $d\delta/dt \approx V_x$, we define the equation of thinning of the interfacial film in the form

$$\frac{d\delta}{dt} = \frac{2g\Delta P}{3\pi\eta R_K^4}\delta^3 + \frac{2\delta^2}{3\eta R_K^2\sin\theta}\frac{\partial\sigma}{\partial\theta} \tag{17}$$

For ΔP we define the following expression $\Delta P = (P_D + P_K)\pi R_K^2 + \Pi$, where P_D, P_K is the dynamic and capillary pressure $\left(P_K = 2\sigma/g\delta\right)$ acting in the film; Π is the wedging pressure, defined both for a spherical drop and $\Pi = -\frac{AR_k^2}{6\delta^3}$ for deformable drops; and A is the van der Waals-Hamaker constant $\left(A \sim 10^{-21}J\right)$ [23, 24].

Given the foregoing, the equation of thinning of the interfacial film (17) can be represented as

$$\begin{aligned} \frac{d\delta}{dt} = b_1\delta^3 + b_2\delta^2 - b_3\delta, \\ t = 0, \delta = \delta_0 \end{aligned} \tag{18}$$

where $b_1 = \frac{2gP_D}{3\eta R_K^4}$, $b_2 = \frac{2}{3\eta R_K^2}\left(2\sigma + \frac{1}{\sin\theta}\frac{\partial\sigma}{\partial\theta}\right)$, and $b_3 = \frac{1}{9}\frac{Aa_r g}{\pi\eta R_K^4}$. The general solution of Eq. (18) will be presented in the form of a transcendental expression:

$$\ln \frac{\delta^2}{\delta_0^2} \frac{b_1\delta_0^2 + b_2\delta_0 - b_3}{b_1\delta^2 + b_2\delta - b_3} - \frac{b_2}{\sqrt{\Delta}} \ln \frac{\left(2b_1\delta + b_2 - \sqrt{\Delta}\right)\left(2b_1\delta_0 + b_2 + \sqrt{\Delta}\right)}{\left(2b_1\delta + b_2 + \sqrt{\Delta}\right)\left(2b_1\delta_0 + b_2 - \sqrt{\Delta}\right)} = -2b_3 t \tag{19}$$

where $\Delta = \frac{2}{9\eta^2 R_K^2}\left[\frac{g^2 P_D A a_r}{\pi R_K^4} + 2\left(\frac{\sigma}{3} + \Delta\sigma\right)^2\right]$. Solution (19) is a complex expression for determining the change in the thickness of an interfacial film $\delta(t)$, in connection with which we consider more specific cases:

a. For thin films, we can put that $P_D << P_K - \Pi/\pi R_K^2$. In this case, the solution of Eq. (18) will be presented as a special case (19):

$$\delta(t) = \frac{\delta_0 \exp(b_3 t)}{1 + \beta_1\delta_0(\exp(b_3 t) - 1)} \tag{20}$$

where $\beta_1 = \frac{b_2}{b_3} = \frac{6\pi R_k^2}{A a_r g}\left(2\sigma + \frac{1}{\sin\theta}\frac{\partial\sigma}{\partial\theta}\right)$. For very thin films, solution (18) appears as

$$\delta(t) \approx \delta_0 \exp(-b_3 t) \tag{21}$$

where $\beta_3 = \frac{2}{3}\frac{P_D g \delta_0}{\eta R_K^2}$. In the case of deformable drops, we have

$$\delta(t) \approx \delta_0 - \beta_2 t \tag{22}$$

where $\beta_2 = \frac{Ag}{9\pi\eta\delta_0 R_K^2}$.

b. For thick films, we can put that $(P_D + P_K) >> \Pi/\pi R_K^2$. It is important to note that the main forces determining the discontinuity of the interfacial film at its large thicknesses are the forces due to velocity pulsations, i.e., hydrodynamic forces. Provided that $P_D >> P_K$, the decision is presented in the form

$$\delta(t) = \frac{\delta_0}{\sqrt{1 + \beta_3 t}} \tag{23}$$

If $P_D << P_K$, then we have

$$\delta(t) = \frac{\delta_0}{1 + b_2\delta_0 t} \tag{24}$$

The above solutions (20)–(24) can be used in practical calculations of the thickness of the interfacial film for special cases. As follows from Eq. (20), the Marangoni effect is a partial correction to the surface tension coefficient in the coefficient b_2, although it can have a significant effect on the nature of the flow and on the velocity distribution in the interfacial films (12) and (16).

It should be noted that various chemical reagents and demulsifiers significantly reduce the surface tension of the film and significantly increase the rate of thinning of the interfacial film (**Figure 3**).

Figure 4 shows a comparison of experimental and calculated values according to Eq. (17) for thinning the film thickness, and after reaching the critical value thickness $\delta \leq \delta_{cr}$, the calculation according to formula (24) is most acceptable.

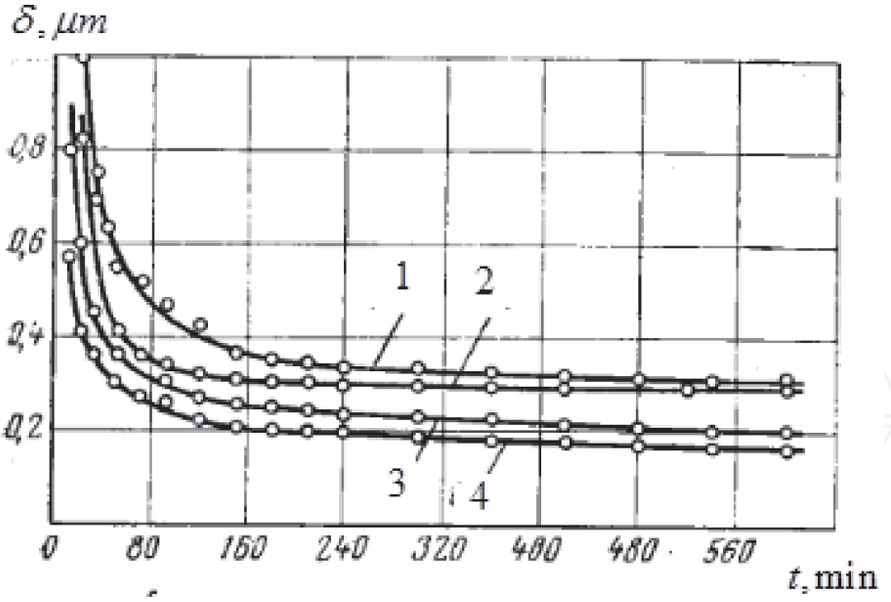

Figure 3.
Change in the thickness of the interfacial film for various concentrations of demulsifier (g/l): 1, 0.02; 2, 0.01; 3, 0.005; 4, 0.002.

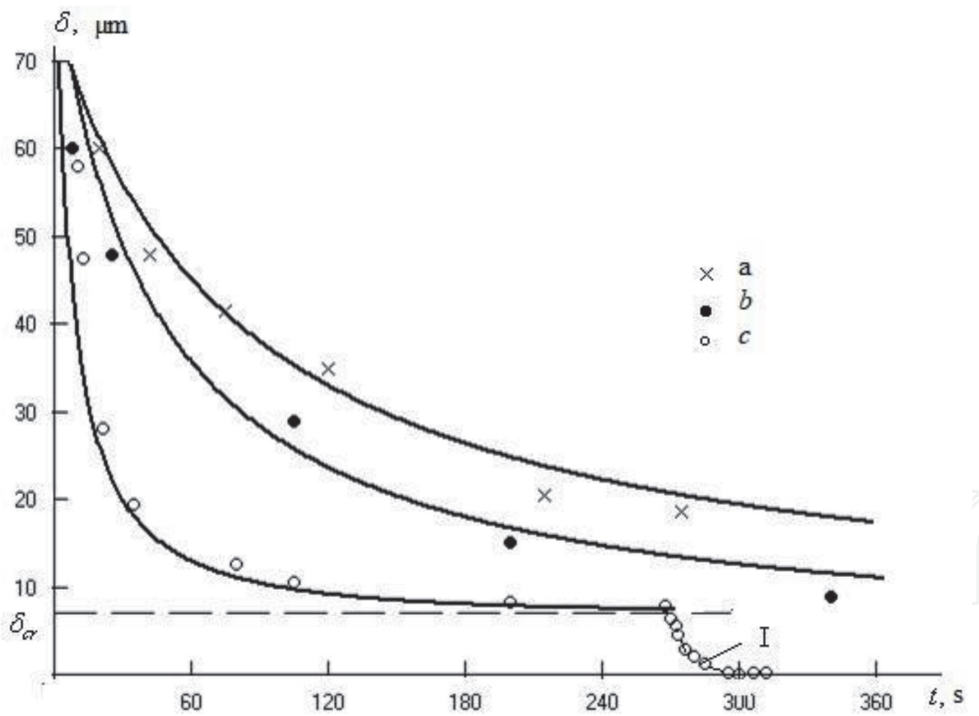

Figure 4.
Comparison of the calculated (17) and experimental values [25] of the thickness of the interfacial film versus time at various concentrations (g/l) of the demulsifier (g/l): a, *0.2;* b, *0.5;* c, *1.0 (I, calculation according to Eq. (24)).*

2.3 Coalescence, deformation, and crushing of droplets in an isotropic turbulent flow

The processes of coalescence and fragmentation of droplets are reversible phenomena and can be described by similar equations.

The crushing of droplets and bubbles in an isotropic turbulent flow is an important factor for increasing the interfacial surface and the rate of heat and mass transfer in dispersed systems. The crushing mechanism of deformable particles is determined by many factors, among which it is important to note the following:

a. The effect of turbulent pulsations of a certain frequency on the surface of droplets and bubbles on the change in shape.

b. Boundary instability on the surface of the droplet, determined by the turbulization of the boundary layer or general instability as a result of reaching the droplet size maximum value $a \geq a_{\max}$.

c. The influence of the external environment, in which the droplet crushing is defined as the equilibrium between the external forces from the continuous phase (dynamic pressure) and the surface tension forces that resist the destruction of the droplet. It should be noted that this condition can also characterize the deformation of the shape of drops and bubbles.

d. As a result of mutual elastic collision with intensive mixing of the system. It is important to note that not every collision of droplets and bubbles leads to their coalescence and coalescence, and during an elastic collision, a droplet can decay into fragments, thereby changing the size distribution spectrum, although there is no work indicating the number of particles formed as a result of such decay.

A general review of the fragmentation of droplets and bubbles is given in the work [26], where issues related to the frequency of crushing and the nature of the particle size distribution function are considered, although the analysis of the maximum and minimum sizes and the characteristic features of the effect of secondary crushing processes on the change in the function of the multimodal distribution of drops are not considered. Despite the many mechanisms for crushing droplets and bubbles, an important parameter characterizing this process is the frequency of crushing in a turbulent flow, the definition of which has been the subject of many works. It should be noted that the mechanisms of coalescence and fragmentation of droplets are similar and differ only in the dependence of energy dissipation on the number of particles. Based on the analysis of surface energy and kinetic energy of a turbulent flow, the following expression is proposed for the droplet crushing frequency [26]:

$$\omega(a) = C_1 a^{-2/3} \varepsilon_R^{1/3} \exp\left(-\frac{C_2 \sigma}{\rho_c \varepsilon_R^{2/3} a^{5/3}}\right) \tag{25}$$

In an isotropic turbulent flow, coalescence and fragmentation of droplets are determined by their turbulent diffusion, represented as [18, 27].

$$\begin{aligned} D_T &\approx \alpha(\varepsilon_R/\lambda)^{1/3}\lambda, \quad \lambda > \lambda_0 \\ D_T &\approx \alpha(\varepsilon_R/\lambda)^{1/2}\lambda^2, \quad \lambda < \lambda_0 \end{aligned} \tag{26}$$

The process of coalescence and crushing can be considered as a mass transfer process, in connection with which, the change in the number of particles taking into account the diffusion coefficients at $\lambda > \lambda_0$ and Pe $<<$1 can be written as [7–10].

$$\begin{aligned}&\frac{\partial N}{\partial t}=\frac{\alpha}{r^2}\frac{\partial}{\partial r}\left[\mu_P^2\varepsilon_R^{1/2}r^{10/3}\frac{\partial N}{\partial r}\right]\\&t=0, r>R, N=N_0\\&t>0, r=R, N=0\\&r\to\infty, N=N_0\end{aligned}\tag{27}$$

The general solution of this boundary value problem under certain assumptions will be presented as

$$\begin{aligned}N(r,t)&=\sum_{n=1}^{\infty}A_nJ_2\left[\mu_n(r/R)^{1/3}\right]\exp\left(-\mu_n^2t\right)\\A_n&=\frac{2}{R^2}\frac{\int_0^R N_0J_0\left(\mu_n(r/R)^{1/3}\right)rdr}{J_1^2\left(\mu_n^2\right)}\end{aligned}\tag{28}$$

The frequency of coalescence and crushing is defined as

$$\omega=D_T\frac{\partial N}{\partial r}|_{r=R}\approx C_1\left(\frac{\varepsilon_R}{a^2}\right)^{1/3}\exp\left(-C_2\left(\varepsilon_R/a^2\right)^{1/3}t\right)\tag{29}$$

We introduce the relaxation time for the coalescence of droplets in a turbulent flow in the form

$$\begin{aligned}&\lambda>\lambda_0,\quad \tau_{PT}=\left(\frac{a^2}{\varepsilon_R}\right)^{1/3}\\&\lambda<\lambda_0,\quad \tau_{PT}=\left(\frac{\nu_c}{\varepsilon_R}\right)^{1/2}\end{aligned}\tag{30}$$

Then the coalescence frequency is defined as

$$\omega=D_T\frac{\partial N}{\partial r}|_{r=R}\approx C_1\left(\frac{\varepsilon_R}{a^2}\right)^{1/3}\exp\left(-C_2t/\tau_{PT}\right)\tag{31}$$

Thus, if $t<<\tau_{PT}$ rapid coalescence and droplet coalescence occur, as a result of which we have

$$\omega=C_1\left(\frac{\varepsilon_R}{a^2}\right)^{1/3}\tag{32}$$

Similarly, it is possible to determine the frequency of coalescence and crushing at $\lambda<\lambda_0$ using the second Eq. (26); for the diffusion coefficient for a viscous flow, the crushing frequency can be determined by the following expression:

$$\omega(a)=C_{01}N_0a^3\left(\frac{\varepsilon_R}{\nu_c}\right)^{1/2}\exp\left[\frac{\sigma}{\left(\nu_c\varepsilon_R\right)^{1/2}a\rho_c}\right]\tag{33}$$

As follows from this equation, the frequency of fragmentation of droplets and bubbles in a viscous region or in a liquid medium is inversely proportional to the viscosity of the medium $\sim\nu_c^{-1/2}$, and the time for crushing droplets is taken in the form $\tau\sim\sigma/(\rho_c\varepsilon_Ra)$, although in [18] it is defined as $\tau\sim a^{2/3}\varepsilon_R^{-1/3}$. For processes of

droplet crushing with the number of particles N_0 in a turbulent flow, the droplet crushing frequency for a high droplet crushing rate, these expressions are simplified to the form $t << (a^2/\varepsilon_{RD})^{1/3}$

$$\omega_D(a) \approx C_1 \mu_p^2 N_0 a^3 \left(\frac{\varepsilon_{RD}}{a^2}\right)^{1/3}, \lambda > \lambda_0 \tag{34}$$

or for a viscous flow $t << (\nu_c/\varepsilon_{RD})^{1/2}$

$$\omega_D(a) \approx C_2 \mu_p^2 N_0 a^3 \left(\frac{\varepsilon_{RD}}{a^2}\right)^{1/2}, \lambda < \lambda_0 \tag{35}$$

With an increase in the concentration of the dispersed phase, particle collisions occur, accompanied by the phenomena of coagulation, crushing, and the formation of coagulation structures in the form of a continuous loose network of interconnected particles. With an increase in particle concentration, the effective viscosity increases linearly if the particles of the dispersed phase are distant from each other at sufficiently large distances that exclude intermolecular interaction and are rigid undeformable balls.

In a number of works, depending on the crushing mechanism, the following formulas are proposed for the crushing frequency [28–32]:

$$\omega(a) = C_3 a^{-2/3} \varepsilon_R^{1/3} \left(\frac{2}{\sqrt{\pi}}\right) \Gamma\left(\frac{3}{2} \frac{C_4 \sigma}{\rho_c \varepsilon_R^{2/3} a^{5/3}}\right),$$

$$\omega(a) = C_5 \varepsilon_R^{1/3} erfc\left(\sqrt{C_6 \frac{\sigma}{\rho_c \varepsilon_R^{2/3} a^{5/3}} + C_7 \frac{\eta_d}{\sqrt{\rho_c \rho_d \varepsilon_R^{1/3} a^{4/3}}}}\right), \tag{36}$$

$$\omega(a) = \frac{a^{5/3} \varepsilon_R^{19/15} \rho_c^{7/5}}{\sigma^{7/5}} exp\left(-\frac{\sqrt{2}\sigma^{9/5}}{a^3 \rho_c^{9/5} \varepsilon_R^{6/5}}\right), ; \omega(a) = C_8 nerfc\left(C_9 \frac{\sigma^{3/2}}{n^3 d_T^3 \rho_c^{3/2} a^{3/2}}\right)^{1/3}, .$$

The last equation determines the frequency of droplet crushing in the mixing devices and depends on the mixing parameters [20, 33]. For multiphase systems with a volume fraction of droplets φ, the crushing frequency can be determined in the form

$$\omega(a) = \frac{\varepsilon_R^{1/3}}{a^{2/3}(1+\varphi)} \exp\left(-C_{11} \frac{(1+\varphi)^2 \sigma}{\rho_d a^{5/3} \varepsilon_R^{2/3}}\right) \tag{37}$$

The crushing rate of droplets in an isotropic turbulent flow is characterized by the crushing rate constant, defined as

$$\mathrm{Re}_d < 1, \quad k_R = A_0 \frac{\varepsilon_R^{1/3}}{a^{2/3}} \exp\left(-\frac{A_1 \sigma}{\rho_c \varepsilon_R^{2/3} a^{5/3}}\right) \tag{38}$$

$$\mathrm{Re}_d > 1, \quad k_R = A_0 \frac{\rho_c a^{2/3} \varepsilon_R^{1/3}}{\eta_c} \exp\left(-\frac{A_1 \sigma}{\rho_c \varepsilon_R^{2/3} a^{5/3}}\right) \tag{39}$$

In principle, the expression given in brackets characterizes the ratio of surface energy ($E_\sigma \sim \pi a^2 \sigma / a \sim \pi a \sigma$) to turbulent flow energy

$\left(\overline{E}_T \sim \pi a^2(\Delta P), \left(\Delta P_T = C_1 \rho_c (\varepsilon_R a)^{2/3}\right)\right)$ and characterizes the efficiency of the crushing process

$$\frac{E_\sigma}{\overline{E}_T} \sim \frac{\sigma}{\rho_c \varepsilon_R^{2/3} a^{5/3}} \tag{40}$$

Analyzing Eqs. (29)–(31), it can be noted that the crushing frequency in an isotropic turbulent flow for a region $\lambda > \lambda_0$ is mainly determined by turbulence parameters (specific energy dissipation, scale of turbulent pulsations), medium density, surface stress, and for a viscous flow $\lambda < \lambda_0$, in addition, viscosity of the medium. It is important to note that the fragmentation of droplets and bubbles in an isotropic turbulent flow is preceded by a deformation of their shape, and with significant numbers and sufficiently small numbers, they can take on forms that cannot be described. The equilibrium condition between the surface forces and the external forces of the turbulent flow (40) can also characterize the initial conditions of particle deformation. Coalescence of droplets and bubbles plays an important role in the flow of various technological processes of chemical technology and, above all, in reducing the interfacial surface, in the separation of particles of different sizes, accompanied by their deposition or ascent. The mechanism of coalescence of droplets and bubbles is determined by the following steps: (a) mutual collision of particles with a certain frequency in a turbulent flow; (b) the formation of an interfacial film between two drops and its thinning; (c) rupture of the interfacial film and drainage of fluid from one drop to another, merging and the formation of a new drop. Mutual collisions of particles in the flow volume occur for various reasons:

a. Due to convective Brownian diffusion of the finely dispersed component of particles, which is characteristic mainly for laminar flow at low Reynolds numbers.

b. Due to turbulent flow and turbulent diffusion

c. Due to additional external fields (gravitational, electric, electromagnetic, etc.). If the Kolmogorov turbulence scale λ_0 is smaller or comparable with the size of the droplets in the viscous flow region, then the process is accompanied by a turbulent walk, similar to Brownian, which results in the appearance of turbulent diffusion. However, turbulent diffusion may be characteristic of large particle sizes at large distances λ, due to the high intensity of turbulent pulsations and the heterogeneity of the hydrodynamic field.

d. Due to the effect of engagement as a result of convective transfer of small particles in the vicinity of the incident large particle. As a result of the deposition or ascent of large particles, due to the formation of a hydrodynamic wake, the capture of small particles by large particles significantly increases, which leads to gravitational coalescence if they fall along lines close to the center line. For the processes of droplet coalescence, the capture coefficient plays an important role, which determines the deviation of the real particle capture cross section from the geometric

$$\vartheta = \frac{I}{\pi (L+R)^2 N_0 V_\infty} \tag{41}$$

where I is the mass flow to the surface of the selected particle, ϑ is the capture coefficient, L is the characteristic distance scale, and V_∞ is the velocity of the

medium unperturbed by the sphere of flow. The relationship between the Sherwood number and the capture coefficient in convective diffusion has the form

$$Sh = \frac{1}{2} Pe\vartheta \left(1 + \frac{R}{L}\right)^2$$

The capture coefficient is defined as

$$\begin{aligned} \vartheta &\approx \frac{4}{\mathrm{Pe}} \left(1 - \frac{N_L}{N_0}\right) b_* (1 + b_0 \mathrm{Pe}), \mathrm{Pe} << 1; \\ \vartheta &\approx \left(1 - \frac{N_L}{N_0}\right) \mathrm{Pe}^{-2/3} \left(1 + 0.73 \mathrm{Pe}^{-1/3}\right), \mathrm{Pe} >> 1 \end{aligned} \tag{42}$$

Here N_L is the concentration of particles on the surface of a sphere of radius $r = L$, b_i coefficients;

e. Due to the heterogeneity of the temperature and pressure fields, which contribute to the appearance of forces proportional to the temperature and pressure gradients and acting in the direction of decreasing these parameters. As a result of the action of these forces, the finely dispersed component of the dispersed flow is characterized by their migration due to thermal diffusion and barodiffusion, which also contributes to their collision and coalescence.

f. In addition to the indicated phenomena, physical phenomena (droplet evaporation, condensation) contribute to coalescence, accompanied by the emergence of a hydrodynamic repulsive force (Fassi effect) of the evaporating droplets due to evaporation (Stefan flow) or when the droplet condenses by the appearance of a force acting in the opposite direction. For an inviscid flow and a fast droplet coalescence rate $t << \left(a^2/\varepsilon_{RK}\right)^{1/3}$, expressions (29) and (31) are transformed

$$\omega_K(a) \approx C_1 \mu_p^2 N_0 a^3 \left(\frac{\varepsilon_{RK}}{a^2}\right)^{1/3}, \lambda > \lambda_0 \tag{43}$$

or for a viscous flow $t << \left(\nu_c/\varepsilon_{RK}\right)^{1/2}$

$$\omega_K(a) \approx C_2 \mu_p^2 N_0 a^3 \left(\frac{\varepsilon_{RK}}{\nu_c}\right)^{1/2}, \lambda < \lambda_0 \tag{44}$$

where $\lambda_0 = \left(\nu_c^3/\varepsilon_R\right)^{1/4}$ is the Kolmogorov scale of turbulence and ε_R is the specific energy dissipation in the fluid flow and dispersed medium in the presence of coalescence (ε_{RK}) or fragmentation of particles (ε_{RD}), depending on the number of particles in the flow and on their size. These expressions for a two-particle collision of the i–th and j–th drops can be transformed to the form

$$\begin{aligned} \omega_K(a) &\approx C_1 \mu_p^2 N_0 \left(\frac{\varepsilon_{RK}}{\alpha^2}\right)^{1/3} \left(a_i^2 + a_j^2\right)^{3/2}, \lambda < \lambda_0 \\ \omega_K(a) &\approx C_2 \mu_p^2 N_0 \left(\frac{\varepsilon_{RK}}{\nu_c}\right)^{1/2} \left(a_i^2 + a_j^2\right)^{3/2}, \lambda < \lambda_0 \end{aligned} \tag{45}$$

As follows from this expression, the collision frequency of particles is inversely proportional to their size $\omega \sim a^{-2/3}$ and increases with increasing concentration of

particles in the volume. In these equations (43) μ_p^2 there is a degree of entrainment of particles by a pulsating medium, and for drops of small sizes $\mu_p^2 \to 1$, and for large drops – $\mu_p^2 \to 0$. As follows from formula (45), with increasing viscosity of the medium and particle size, the collision frequency of particles in an isotropic turbulent flow decreases, and, naturally, the probability of the formation of coagulation structures is extremely low. For large Peclet numbers Pe> > 1, using stationary solutions of the convective diffusion equation for fast coagulation, the coalescence frequency can be expressed as

$$\omega_k = C_1 N_0 \left[\left(\frac{\varepsilon_r}{\nu_c}\right) aU\right]^{1/2} a^2 \tag{46}$$

where $C_1 = 8\sqrt{\frac{\pi}{3}}\mu_p^2 a$.

By introducing the Peclet number for isotropic turbulence in the form $\mathrm{Pe} = \frac{U_\infty}{a}\left(\frac{\nu_C}{\varepsilon_R}\right)^{1/2}$, this expression can be rewritten in the form

$$\omega_K = C_1 N_0 U a^2 \mathrm{Pe}^{-1/2} \tag{47}$$

Thus, with an increase in the number Pe, the number of particle collisions decreases, which prevents the formation of coagulation structures. For finely dispersed particles, the number Pe can be expressed as $\mathrm{Pe} = \frac{a}{D}\dot{\gamma}$, which, for isotropic turbulence, is transformed to a form $\mathrm{Pe} = a_1\left(\frac{\nu_C}{\varepsilon_R}\right)^{1/2}\dot{\gamma} = a_1\left(\frac{\eta_C}{\varepsilon_R \rho_C}\right)^{1/2}\frac{\tau}{\eta_C}$, i.e., the Pe number is proportional to the shear stress. Therefore, with $\tau \to \tau_P$, the number Pe becomes infinitely large, which creates the conditions for the formation of coagulation structures.

Coalescence of droplets and bubbles is characterized by the following stages: rapprochement and collision of droplets of different sizes in a turbulent flow with the formation of an interfacial film between them. It should be noted that the transfer of droplets in a polydisperse medium is mainly determined by the hydrodynamic conditions and the intensity of the flow turbulence. Under conditions of isotropic turbulence, the collision frequency of droplets depends on the specific dissipation of the energy of the turbulent flow and the properties of the medium and the dispersed phase.

2.4 Deformation of drops and bubbles

The deformation of droplets and bubbles, first of all, is characterized by a violation of the balance of external and surface stresses acting on the droplet in a turbulent flow. In the simplest case, with insignificance of gravitational and resistance forces, such forces are hydrodynamic head and surface tension. The pressure forces are proportional to the velocity head $F_D \sim \frac{\rho_c U}{2}$, and the surface tension force is proportional to capillary pressure $F_\sigma = \frac{2\sigma}{a_e}$. If the Weber number $We \sim \frac{F_D}{F_\sigma} < < 1$, then for small numbers $\mathrm{Re}_d < < 1$, drops and bubbles have a strictly spherical shape. Under the condition of $F_D \geq F_\sigma$ either $We \geq 1$, $\mathrm{Re}_d > 1$ the surface of the droplet loses stability and it deforms, taking the shape of a flattened ellipsoid of revolution at the beginning, and with a further increase in the number Re_d and We, it assumes various configurations up to the stretched filament, which are not amenable to theoretical investigation and description (**Figure 5**). It should be noted that in dispersed systems, there is a certain maximum size a_{max}, above which the droplets are unstable, deform, and instantly collapse, and the minimum size a_{min}, which

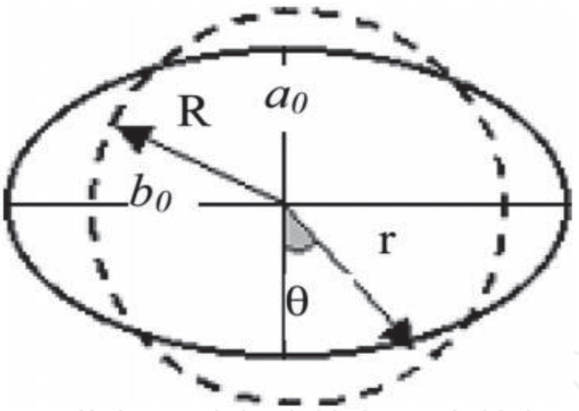

Figure 5.
Schematic representation of the deformation of a drop to an ellipsoidal shape.

determines the lower threshold for the stability of droplets; i.e., under certain conditions, the flows of droplets that have reached these sizes cannot be further fragmented. The maximum particle size characterizes the unstable state of droplets and bubbles, which depend on the hydrodynamic conditions of the dispersed medium flow and, under certain turbulent flow conditions, are prone to shape deformation and fragmentation of a single drop. Usually, deformation of a drop's shape to an ellipsoidal shape is estimated by the ratio of the small axis of the ellipsoid to the large $\chi = a_0/b_0$.

The volumetric deformation of droplets and bubbles is based on a three-dimensional model and results in a change in the shape of a spherical particle to an ellipsoidal one. Moreover, the drop is subjected to simultaneous stretching and compression with a constant volume. In the literature there are a large number of empirical formulas describing the deformation of drops and bubbles. Compared to multidimensional deformation, volumetric deformation is the simplest case with the preservation of a certain shape symmetry (**Figure 6**).

It is important to note that for any deformation of the droplet shape, the surface area of the particle increases with a constant volume of liquid in the droplet, which is an important factor in increasing the interfacial surface.

In [8, 18], the fluctuation frequency of oscillations of the droplet surface using the Rayleigh equation as a result of the influence of turbulent pulsations of a certain frequency on the surface of droplets and bubbles on the shape change is defined as

$$\omega(k) = \left[\left(\frac{2\sigma}{\pi 2\rho_c a^3}\right)\left(\frac{(k+1)(k+2)k(k\text{-}1)}{(k+1)_{\rho d/\rho c}+1}\right)\right]^{1/2} \tag{48}$$

where is k the wave number. For k = 2 using this formula, one can obtain formulas for determining the frequency corresponding to the fragmentation of

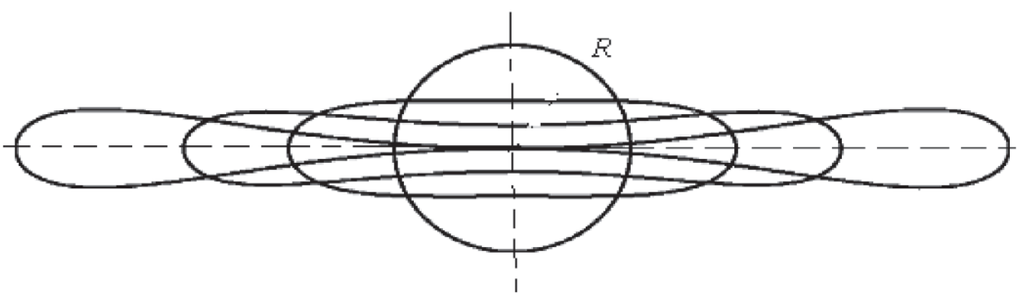

Figure 6.
The characteristic forms of deformation of a spherical drop and bubble.

bubbles $(\rho_d << \rho_c)$ $\omega(a) = \frac{2\sqrt{6}}{\pi}\left(\frac{\sigma}{\rho_c a^3}\right)^{1/2}$ and drops $(\rho_d >> \rho_c)$ $\omega(a) = \frac{4}{\pi}\left(\frac{\sigma}{\rho_d a^3}\right)^{1/2}$. As a result, for minor deformations, the droplet shape is determined by the superposition of linear harmonics

$$r(t,\theta) = R\left[1 + \sum_k A_k \cos(\omega_k t) P_k(\cos\theta)\right] \tag{49}$$

where $P_k(\cos\theta)$ is the Legendre function; Ak are the coefficients of the series, defined as $A_k = A_{k0}\exp(-\beta_k t)$; and β_k is the attenuation coefficient, defined as

$$\beta_k = \frac{(k+1)(k\text{-}1)(2k+1)\eta_d + k(k+2)(2k+2)\eta_c}{[\rho_d(k+1) + \rho_c k]R^2}$$

Expression (49) for small numbers Re_d is represented as

$$r(t,\theta) = R[1 + \xi(\cos\theta)] \tag{50}$$

where $\xi(\cos\theta) = \lambda_m Ac\,\mathrm{Re}_d^2 P_2(\cos\theta) - \frac{3}{70}\lambda_m\frac{11+10\gamma}{1+\gamma}Ac^2\,\mathrm{Re}_d^3 P_3(\cos\theta) + \ldots,$ and R is the radius of the spherical particle. Here $\lambda m = \varphi(\gamma)$, and in particular for gas bubbles in an aqueous medium $\lambda_m = 1/4$, for drops of water in air $\lambda_m \to 5/48$, etc. Putting that

$We = Ac\,\mathrm{Re}_d^2$ we get

$$\xi(\cos\theta) = \lambda_m We P_2(\cos\theta) - \frac{3}{70}\lambda_m\frac{11+10\gamma}{1+\gamma}We^2\,\mathrm{Re}_d^{-1}P_3(\cos\theta) + \ldots. \tag{51}$$

As a parameter characterizing the deformation of droplets and bubbles, we consider the ratio of the minor axis of the ellipsoid a to the major b, i.e., $\chi = a/b$. Having plotted that for $\theta = 90^\circ, P_2(\cos 90^\circ) = -0.5, P_3(\cos 90^\circ) = 0$, from Eqs. (50) and (51), we can write $a = R(1 + a_0 We)$, and for $\theta = 0^\circ, P_2(\cos 0) = 1.0, P_3(\cos 0) = -1$ we define $b = R\left(1 + \beta_0 We + \beta_0 We^2\right)$, where $a_0 = 0.5\lambda m$, $\beta_0 = \lambda_m, \beta_1 = \frac{3}{70}\lambda_m\frac{11+10\gamma}{1+\gamma}\,\mathrm{Re}_d^{-1}$.

Then, putting that $\chi = a/b$, we finally obtain the expression for the dependence of the degree of deformation on the number We in the form

$$\chi = \frac{1 + a_0 We}{1 + \beta_0 We + \beta_1 We^2} \tag{52}$$

where We is the Weber number. This expression is characteristic for describing small deformations of droplets. As a result of using experimental studies [33] on the deformation of the shape of bubbles in a liquid medium with different numbers Mo and to expand the field of application of Eq. (51), the following expression is proposed:

$$\chi = \frac{1 + 0.06We}{1 + 0.2We + \beta_1 We^2} \tag{53}$$

where $\beta_1 = 0.005(2 - \ln Mo)$ with a correlation coefficient equal to $r^2 = 0.986$. **Figure 7** compares the calculated values according to Eq. (53) with experimental data [33].

As follows from **Figure 8**, expression (53) satisfactorily describes the deformation of droplets and bubbles for the region of variation $We < 10$ and $10^{-4} \leq Mo \leq 7$.

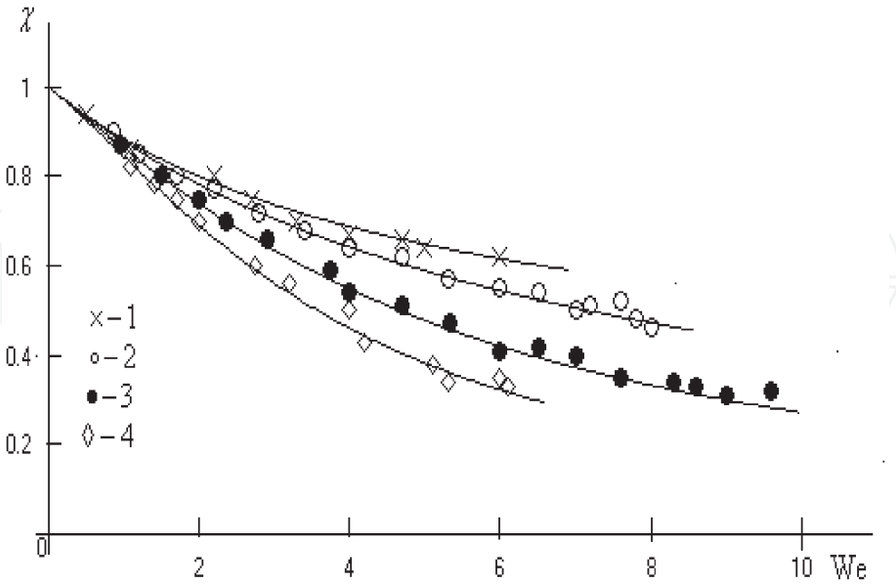

Figure 7.
Dependence of the degree of deformation on the number for various numbers equal to 1, 7; 2, 1.4; 3, 0.023; 4, 0.0001.

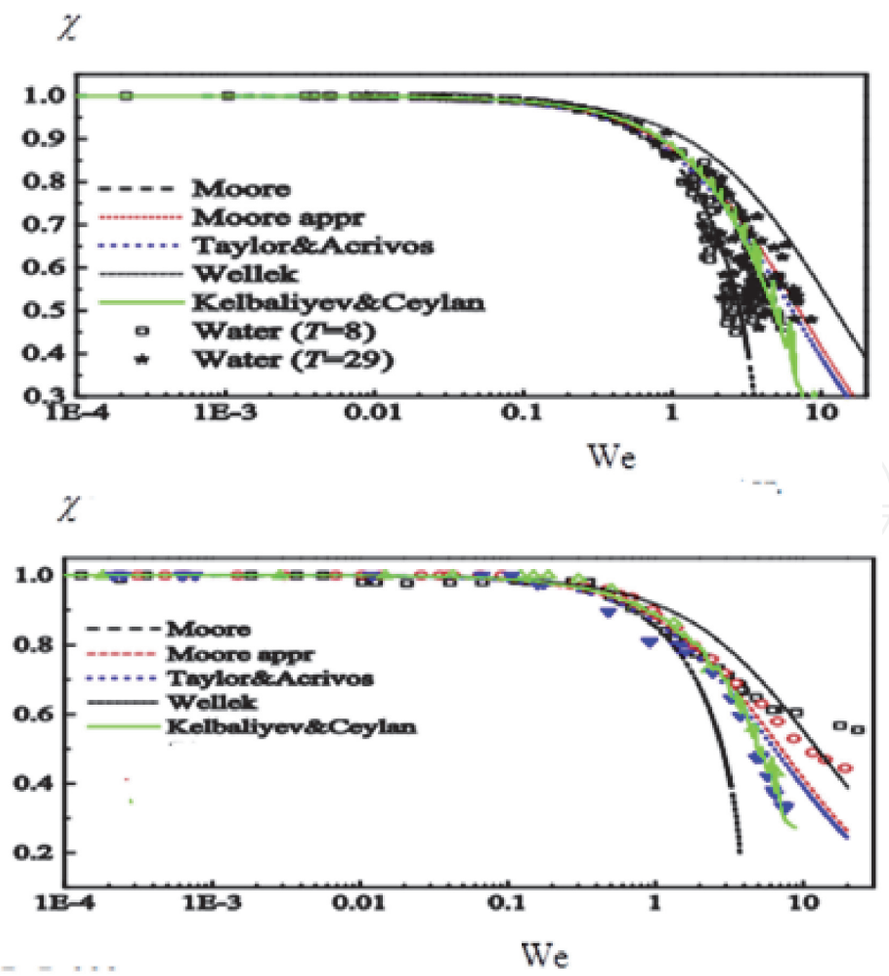

Figure 8.
Comparison of the deformation model (56) of water droplets (pure water in the first graph, glycerol in the second graph) with existing models and experimental data.

Considering only the first term of expression (53) and setting that $P_2(\cos\theta) = 0.5(3\cos^2\theta\text{-}1)$, we obtain

$$r = R\left[1 - \frac{\lambda_0}{2} We(3\cos^2\theta - 1\right] \tag{54}$$

If $\theta = 0$ and $r = a_0$, then expression (54) can be written as

$$a_0 = R(1\text{-}\lambda_0 \mathrm{We}) \tag{55}$$

and if $\theta = \pi/2$ and $r = a_0$, then we have $b_0 = R(1 + \lambda_0/2We)$. Then the relative deformation of the drop is defined as

$$\chi = \frac{a_0}{b_0} = \frac{1 - \lambda_0 We}{1 + (\lambda_0/2)We} \tag{56}$$

Here λ_0, the parameter is determined empirically, using experimental data in the form

$$\lambda_0 = \frac{1}{12}\left(1 - \frac{3}{25}\frac{We}{\mathrm{Re}_d}\right) \tag{57}$$

In [34], this model was used to study the deformation of drops, and a comparison is made with other existing models, the results of which are shown in **Figure 8**.

The authors of [34] note that model (56) is the best compared to existing models.

3. The structural viscosity of oil emulsions

The structural viscosity of a dispersed medium associated with the content of the dispersed phase, as well as with various physical phenomena of interaction between particles, varies from the molecular viscosity of a Newtonian fluid in the absence of dispersed particles ($\varphi = 0$) to shear or bulk viscosity at high particle concentrations ($\varphi \to \varphi_\infty$). Moreover, as experimental studies have shown, the region of the onset of structure formation is clearly distinguished on the curve of viscosity change. The structural viscosity is influenced by the processes of coagulation of particles, accompanied by the formation of coagulation structures in the form of a continuous grid. In most cases, taking these factors into account results in constructing a viscosity model depending on the volume fraction of particles $\eta = f(\varphi)$ or on the fraction of particles and shear stress $\eta = f(\varphi, \tau)$ and shear rate. The rheological oil models of various fields, reflecting the relationship between stress and shear rate through structural viscosity or consistency, obey different laws, exhibiting different properties: visco-plastic, viscoelastic, or having exponential functions. With an increase in the number of particles per unit volume, the effective viscosity of non-Newtonian oil transforms into structural viscosity, which reflects the nature of the formation of this structure. Under certain conditions, rheological models for oil of various fields can be represented by the equations of Bingham ($\tau = \tau_0 + \eta\dot{\gamma}$), Casson ($\tau^{1/2} = \tau_0^{1/2} + k^{1/2}\dot{\gamma}^{1/2}$), Herschel-Bulkley ($\tau = \tau_0 + k\dot{\gamma}^n$), or many other rheological equations. Despite the wide variety of rheological models, in some cases, different models describe the same experimental measurements with equal accuracy. In

addition, rheological models differ in the nature of the dependence of the effective viscosity on the content of asphaltenes, resins, and paraffin.

3.1 The dependence of the viscosity of oil emulsions on the water content

One of the important rheological parameters of emulsions is their dynamic viscosity, which depends on the volume fraction, size, and shape of the droplets, on the ratio of the viscosity of the droplets to the viscosity of the medium $\lambda = \eta_d/\eta_c$ (mobility of the surface of the droplets), on the shear stress in concentrated emulsions, etc. Viscosity is the main parameter of structured disperse systems that determines their rheological properties. With an increase in particle concentration, the effective viscosity increases linearly if the particles of the dispersed phase are distant from each other at sufficiently large distances that exclude intermolecular interaction and are rigid undeformable balls (**Table 1**).

A large number of empirical formulas for calculating the viscosity of dispersed media are given in the work [40, 41]. At high concentrations of particles in the volume, taking into account the hydrodynamic interaction of particles, some authors use a modification of the Einstein equation

$$\eta_{ef} = \eta_C\left(1 + 2,5\varphi + a_0\varphi^2 + a_1\varphi^3 + \ldots\ldots\right) \tag{58}$$

where a_i are the coefficients that take into account physical phenomena in a dispersed flow, which in different works take different values.

As a semiempirical expression for calculating the effective viscosity of suspensions, which describes the experimental data well over a wide range of particle concentrations, the Moony formula [7, 8] can be noted

$$\eta_{ef}/\eta_C = \exp\left[\kappa_1\phi/(1-\kappa_2\phi)\right] \tag{59}$$

where κ_1 and κ_2 are coefficients equal to $\kappa_1 = 2,5$ and $0,75 \le \kappa_2 \le 1,5$. This formula for $\varphi \to 0$ provides the limit transition to the Einstein formula.

No.	Formulas for viscosity	Links
1	$\eta_{ef} = \eta_c(1 + 2.5\varphi),\ \ \varphi < 0.01$	Einstein's formula
2	$\eta_{ef} = \eta_c(1 + 2.5\varphi + 6.2\varphi^2),\ \ \varphi < 0.1$	[35]
3	$\eta_{ef} = \eta_c\left(1 - \frac{\varphi}{\varphi_\infty}\right)^{-2.5\varphi_\infty},\ \ \varphi_\infty \approx 0.64$	[36]
4	$\eta_{ef} = \eta_c\left(1 - \frac{\varphi}{\varphi_\infty}\right)^{-2}$	[37]
5	$\eta_{ef} = \eta_c\left(1 - \frac{\varphi}{\varphi_\infty}\right)^{-2.5\varphi_\infty \frac{\eta_d + 0.4\eta_c}{\eta_d + \eta_c}}$	[38]
6	$\eta_{ef} = \eta_c \exp\left[2.5\frac{\eta_d + 0.4\eta_c}{\eta_d + \eta_c}\left(\varphi + \varphi^{5/3} + \varphi^{11/3}\right)\right]$	[38]
7	$\eta_{ef} = \eta_c\left(1 + 2.5\varphi\frac{\eta_d + 0.4\eta_c}{\eta_d + \eta_c}\right)$	[38]
8	$\eta_{ef} = \eta_c \exp\left(\frac{2.5\varphi}{1 + k_1\varphi}\right),\quad 0.75 < k_1 < 1.5$	[38]
9	$\eta_{ef} = \eta_c k_1(\varphi/\varphi_\infty)^{1/3}\left[(1 - \varphi/\varphi_\infty)^{1/2} + 1\right]$	[39]
10	$\eta_{ef} = \eta_c k_1\left[1 + 0.75\varphi/\varphi_\infty(1 - \varphi/\varphi_\infty)^{-1}\right]^2$	[39]

Table 1.
Empirical formulas for calculating the effective dynamic viscosity of disperse systems.

Taylor has generalized this equation to the effective viscosity of emulsions

$$\eta_{ef} = \eta_C\left(1 + 2,5\phi\frac{\eta_d + 0,4\eta_C}{\eta_d + \eta_C}\right) \tag{60}$$

where η_d and η_c are the viscosities of the dispersed phase and the medium.

For the effective viscosity of a disperse system, *Ishii and Zuber* offer the following empirical formula

$$\eta_{ef}/\eta_C = \left[1 - \left(\varphi/\varphi_\infty\right)\right]^{-m} \tag{61}$$

where φ_∞ is the volume fraction of particles corresponding to their maximum packing, $\varphi_\infty = 0.5 - 0.74$, and $m = 2.5\varphi_\infty^{(\eta_d+0,4\eta_c)/(\eta_d+\eta_c)}$. In this formula, the value $\varphi_\infty = 0.62$ is the most suitable for most practical cases. *Kumar et al.* [7, 8] for wide limits changes φ from 0.01 to 0.75 suggested the following formula:

$$\frac{\eta_{ef}}{\eta_C} = \exp\left[2.5\frac{0.4\eta_C + \eta_d}{\eta_C + \eta_d}\left(\phi + \phi^{5/3} + \phi^{11/3}\right)\right] \tag{62}$$

This formula was tested for various liquid–liquid systems and gave the most effective result with a relative error of up to 20%. Many models express the dependence of the viscosity of a disperse system on the limiting concentration of particles φ_p, at which the flow stops on the limiting shear stress. In addition to the above models, there are many empirical and semiempirical expressions in the literature for calculating the viscosity of concentrated systems, although the choice of a model in all cases is based not on the structure formation mechanism, but on the principle of an adequate description of experimental data.

In the literature you can find many other rheological models, using which you can give various dependencies to determine the viscosity of the system [7, 8].

$$\frac{\eta_{ef} - \eta_0}{\eta_0 - \eta_\infty} = f(\dot{\gamma}\theta_w),\ \eta = \eta_\infty + \frac{\eta - \eta_\infty}{1 + (\alpha_0\tau)^m},\ \eta = \eta_\infty + \frac{\eta - \eta_0}{1 + \alpha_0\dot{\gamma}^m + \alpha_1\dot{\gamma}} \tag{63}$$

Here $\gamma = \partial V/\partial y^-$ is the shear rate, τ_0 is the limit value of the shear stress, k^- is the consistency coefficient, and η_∞^- is the viscosity for the suspension in the absence of interaction between the particles.

The empirical models presented are used for specific applications and represent formulas for adequate approximation of experimental data, although we note that attempts to find a general rheological equation for different systems are considered impossible in advance. It is important to note that effective viscosity also depends on particle sizes. However, if we assume that the volume fraction of particles per unit volume is equal to $\varphi = N_0\pi a^3/6$ (N_0 is the number of particles per unit volume), then any expressions that allow us to determine the effective viscosity of a dispersed medium in an indirect order through the volume fraction of particles express the dependence of viscosity on particle size. Effective viscosity does not significantly depend on large particle sizes. **Figure 9** shows the dependence of the effective viscosity on the volume fraction of suspension solid particles for their various sizes, calculated by the formula

$$\eta_{ef} = 1 + 2.5\varphi + 1.5\varphi\exp\left(\frac{0.45\varphi}{(\varphi - \varphi_\infty)^2}\right) \tag{64}$$

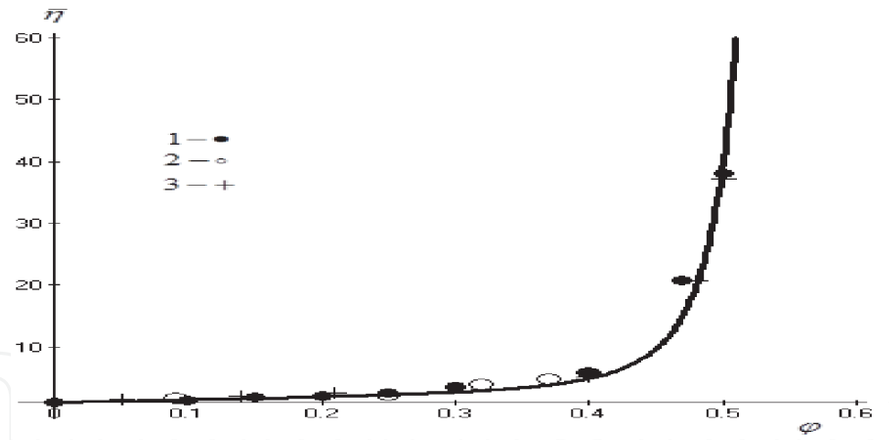

Figure 9.
The dependence of the effective viscosity of suspensions on the fraction of particles and their sizes: 1, 90–105 μm; 2, 45–80 μm; 3, 30–40 μm.

For small particle sizes, the dependence of effective viscosity on particle sizes becomes more noticeable, where the dependence of viscosity on particle sizes is described by the expression

$$\eta_{ef} = 1 + 2,5\varphi + \frac{3}{4}\varphi \exp\left(\frac{m\varphi}{(\varphi - \varphi_\infty)^2}\right), \quad m = 2.2 + 0.03a \tag{65}$$

The correspondence of this dependence to experimental data is shown in **Figure 10**.

As follows from the experimental data and from this formula, the effective viscosity of a dispersed system substantially depends on the volume fraction and particle size. Moreover, with increasing particle size, the effective viscosity also increases. In all likelihood, in this case, coagulation structures and aggregates are not formed, but a simple dense packing of particles is formed.

The effective viscosity of the disperse system grows up to a critical value, which affects the speed and nature of the flow (**Figure 10**). Coagulation structures are formed due to intermolecular bonds between particles, and if liquid interlayers remain between the particles, then the thickness of this interlayer significantly affects the strength of the coagulation structure. The change in the effective viscosity of non-Newtonian oil from the pressure gradient, accompanied by the formation

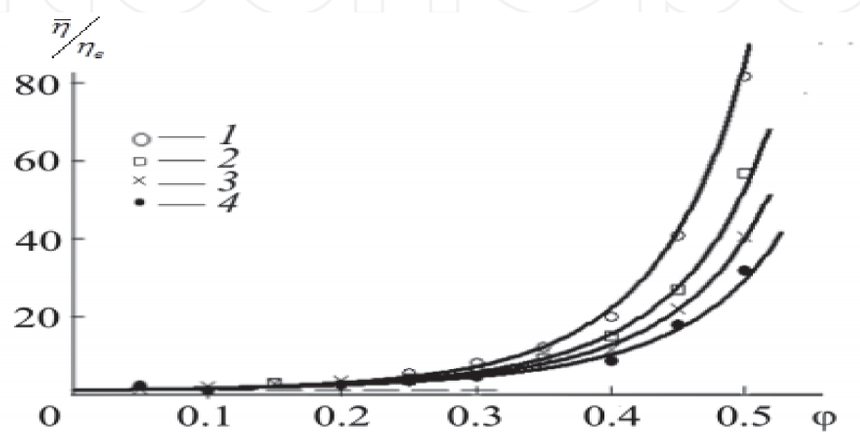

Figure 10.
The calculated (solid curves) experimental (points) of the relative viscosity of the dispersed system from the volume fraction of solid spherical particles and their sizes: 1, a = *0.1 μm; 2, 0.5 μm; 3, 1.0 μm; 4, 1.5 μm.*

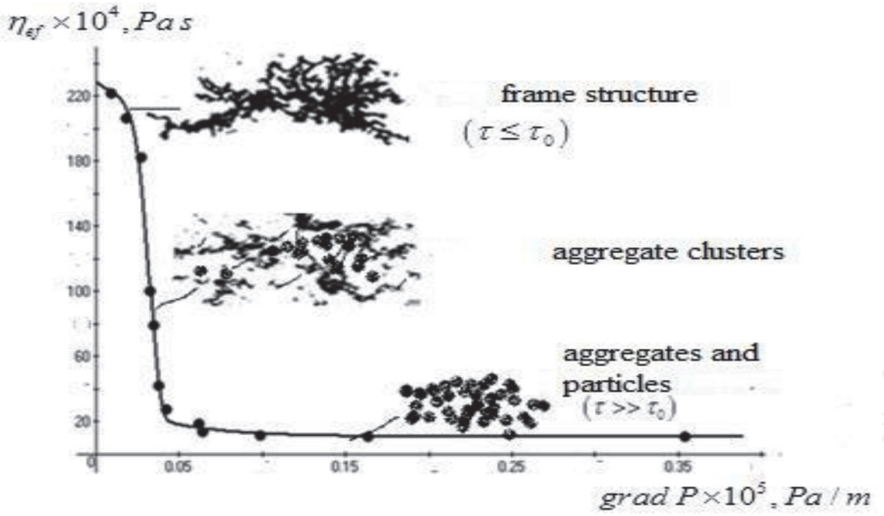

Figure 11.
The dependence of the viscosity of the structured system on the nature of its destruction at various values of the pressure gradient.

and destruction of the structure due to particles of asphaltenes, based on experimental data, is determined by the empirical formula [8, 42].

$$\frac{\eta_{ef} - \eta_\infty}{\eta_0 - \mu_\infty} = \exp\left(-30z^6\right) \tag{66}$$

where η_0, μ_∞ is the initial $(\tau \le \tau_P)$ and final viscosity of the oil $\tau > > \tau_P, z = grad\ P$. **Figure 11** shows the change in the viscosity of the destroyed structure, although the formation of the same structure also occurs only in the opposite direction; i.e., the system is characterized by thixotropy of the structure.

The viscosity of disperse systems also depends on the size and deformation of the particle shape, and with increasing size, the viscosity increases. Despite the large number and variety of viscosity models of disperse systems, the main studies are devoted to the construction of empirical models without taking into account the mechanism of phenomena that describe experimental data with a certain accuracy. The nature and properties of coagulation structures significantly affect the basic properties of a dispersed medium. It is very difficult to determine the viscosity of composite materials, where the formation of certain structures is an important and necessary problem, where the viscosity depends on the concentration of the components included in this system, molecular weight, temperature, and many other parameters.

The viscosity of free-dispersed systems increases with increasing concentration of the dispersed phase. The presence of particles of the dispersed phase leads to a distortion of the fluid flow near these particles, which affects the viscosity of the dispersed system. If the concentration is negligible, then the collision of the particles is excluded, and the nature of the fluid motion near one of the particles will affect the fluid motion near the others.

The work [43] provides a formula for calculating the viscosity of an oil emulsion for its various types

$$\frac{\eta_{ef}}{\eta_C} = \exp(5\varphi)(1 - 3\varphi + b\varphi) \tag{67}$$

Here η_{ef}, η_C are the dynamic viscosities of the emulsion and oil, φ is the volume fraction of droplets, and b is an emulsion type factor, moreover, b = 7.3 for highly

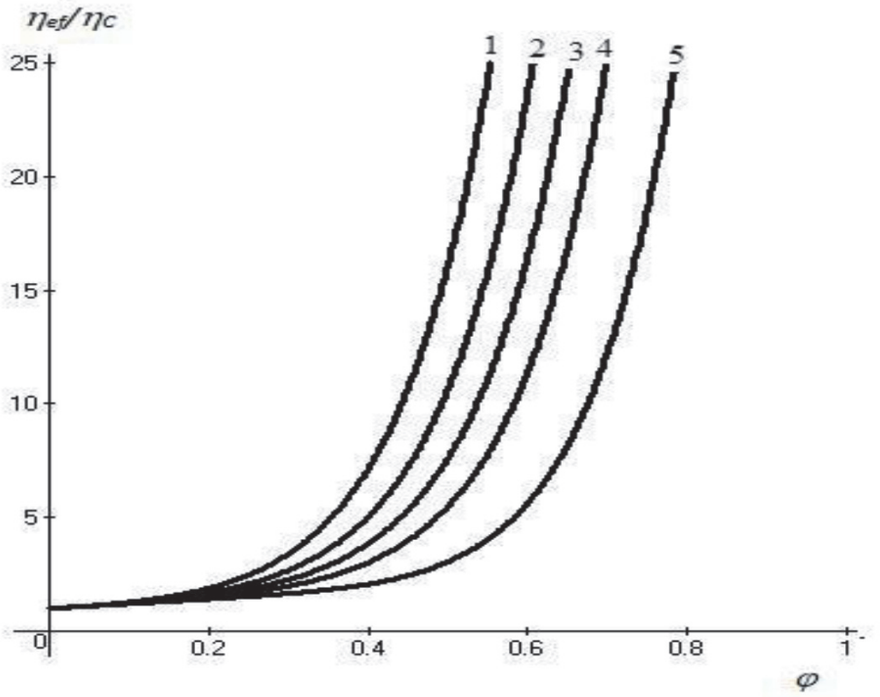

Figure 12.
The dependence of the viscosity of the oil emulsion on the water content: (1) highly concentrated emulsions, b = 7.3; (2) concentrated emulsions, b = 5.5; (3) for average emulsion concentrations, b = 4.5; (4) for diluted emulsions, b = 3.8; (5) for highly diluted emulsions, b = 3.0.

concentrated emulsions, b = 5.5 for concentrated emulsions, b = 4.5 for medium concentration emulsions, b = 3.8 for diluted emulsions, and b = 3.0 for very diluted emulsions. **Figure 12** shows the calculated curves of the dependence of the viscosity of the oil emulsion on the volumetric water content.

It is important to note that, in addition to the above factors, the viscosity of emulsions is associated with the presence of deformable drops and bubbles in them, and at high concentrations of drops with the formation of coagulation structures (flocculus), leading to rheological properties. The work [44] considers possible options for calculating the viscosity of emulsions taking into account structural changes. If we introduce the stress relaxation time in the form

$$\tau = \frac{\eta_C R}{\sigma} \frac{(2\lambda+3)(19\lambda+16)}{40(\lambda+1)} \tag{68}$$

then the viscosity of the emulsions can be calculated by the formula

$$\eta_{ef} = \frac{\eta_C}{1+\left(\tau\dot{\gamma}^2\right)}\left[1+\frac{1+2.5\lambda}{1+\lambda}\varphi+\left(1+\varphi\frac{5(\lambda-1)}{2\lambda+3}\left(\left(\tau\dot{\gamma}^2\right)\right)\right)\right] \tag{69}$$

Here $\gamma = {}^{\eta_d}/_{\eta_C}$ and τ is the shear stress. For small quantities $\tau\dot{\gamma} << 1$, this equation takes the following form

$$\frac{\eta_{ef}}{\eta_C} = \frac{1+2.5\lambda}{1+\lambda}\varphi \tag{70}$$

and, when $\lambda \to \infty$, i.e., for particulate matter, $\eta_{ef}/\eta_C = 1 + 1.25\varphi$. **Figure 13** shows the visual nature of the change in the viscosity of emulsions depending on the shear stress and the volume fraction of drops. The following formula is given in [45]

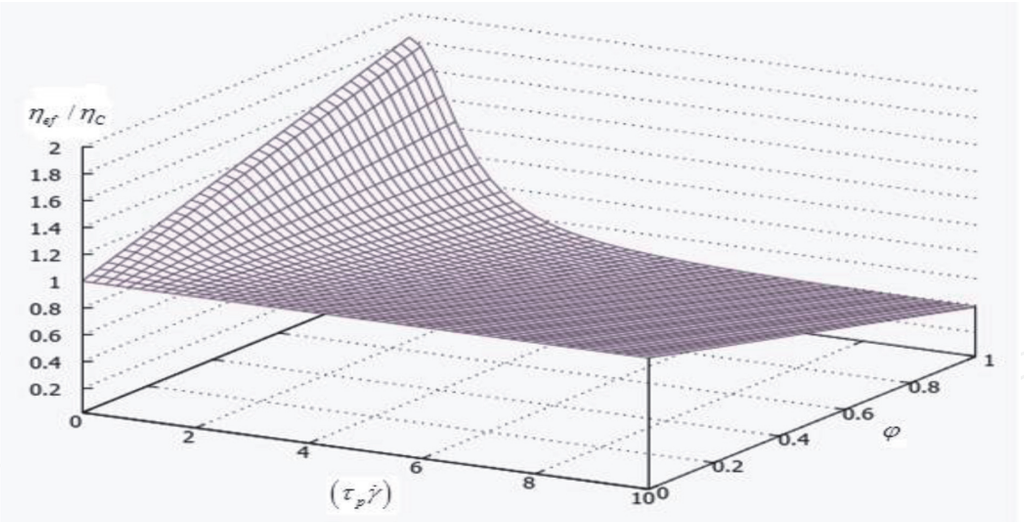

Figure 13.
Spatial interpretation of the nature of the change in viscosity of emulsions at $\lambda = 0.5$.

for calculating the viscosity of monodisperse emulsions depending on the droplet size and their volume fraction

$$\frac{\eta_{ef}}{\eta_C} = 1 + \frac{\eta_C + 2.5\eta_d + (\eta_{ds} + \eta_{di})/a}{\eta_C + \eta_d + 0.4(\eta_{ds} + \eta_{di})/a}\varphi \tag{71}$$

Here η_{ds} is the interfacial shear viscosity, η_{di} is the dilatant viscosity, and a is the droplet size.

3.2 The dependence of the effective viscosity of oil on the content asphaltenes

An experimental study of the effect of the content of asphaltenes and resins in oil on its rheological properties and viscosity was proposed in [46–48].

Using the results of these studies, it can be noted that the presence of asphaltenes, resins, and paraffins in oil, which change the properties of oil, significantly affects their movement and transport. First of all, this affects the stress and shear rate and the increase in viscosity of non-Newtonian oil. In **Figure 14**, the dependence of the effective viscosity of Iranian oil on shear rate by various rheological models is proposed [47].

The table below shows the values of the main coefficients included in these rheological models at various temperatures [47] (**Table 2**).

Of all the models, a satisfactory approximation to the experimental data gives the expression (T = 25°C)

$$\eta = 45.86\dot{\gamma}^{0.75}$$

Given this expression, a rheological dependence satisfying the experimental data can be represented as

$$\tau = \tau_0 + 45.76\dot{\gamma}^{1.75} \tag{72}$$

The dependence of the coefficient of consistency on temperature can be expressed by the following equation:

$$k = 399.2\exp(-0.081T)$$

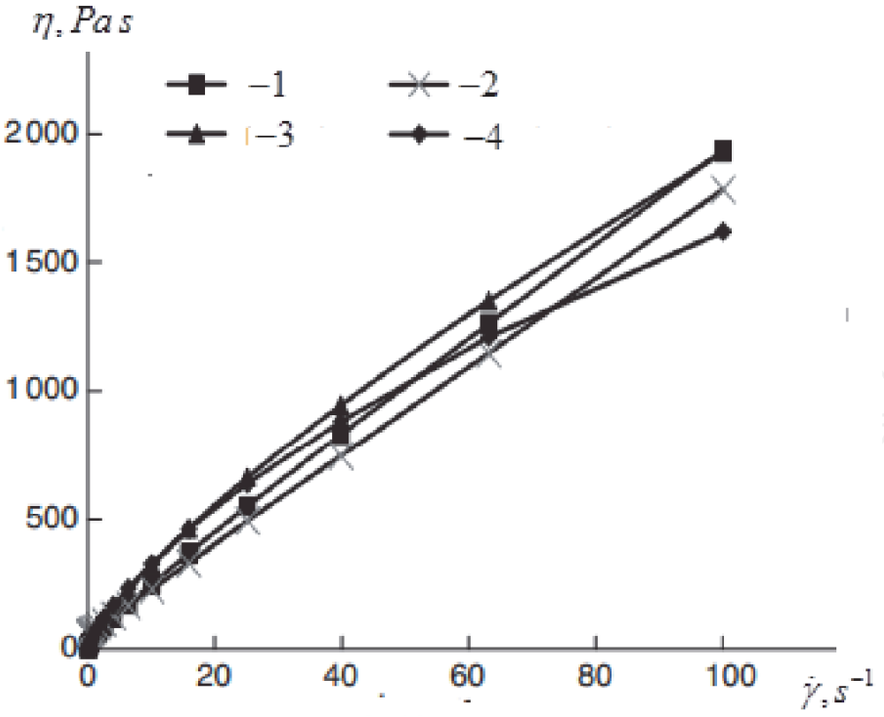

Figure 14.
Approximation of the dependence of viscosity on shear rate by various rheological models: (1) Casson model, $\tau = \left(\tau_0^{1/2} + k^{1/2}\dot{\gamma}^{1/2}\right)^2$*; (2) Bingham model,* $\tau = \tau_0 + \eta\dot{\gamma}$*; (3) exponential function,* $\tau = k\dot{\gamma}^n$*; (4) experiment.*

	Temperature								
	25°C			45°C			60°C		
Model	τ_0, Pa	$k, Pa s$	n	τ_0, Pa	$k, Pa s$	n	τ_0, Pa	$k, Pa s$	n
Casson	8.13	4.11	–	0.57	2.2	–	0.15	1.53	–
Power law	–	54.65	0.77	–	9.26	0.88	–	3.86	0.9
Bingham	61	17.23	–	8.66	4.81	–	3.13	2.33	–

Table 2.
Coefficients of rheological models at T = *25, 45, and 60°C.*

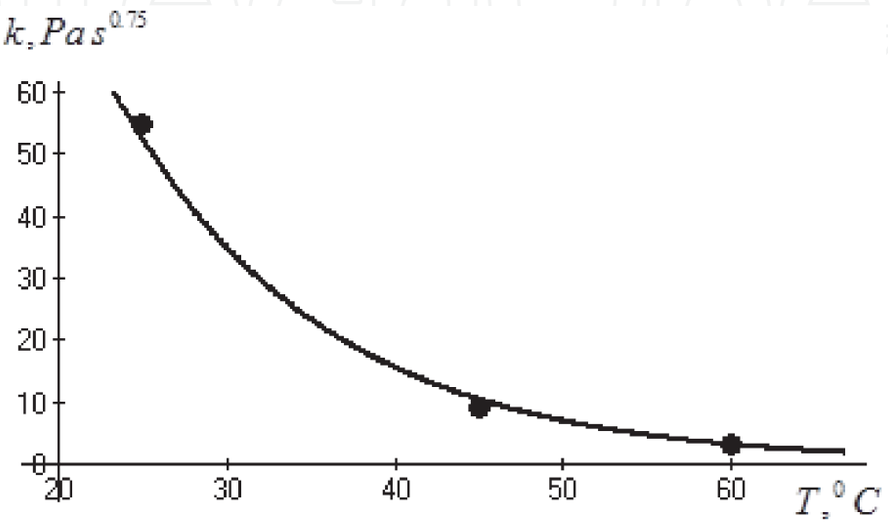

Figure 15.
The dependence of the coefficient of consistency on temperature.

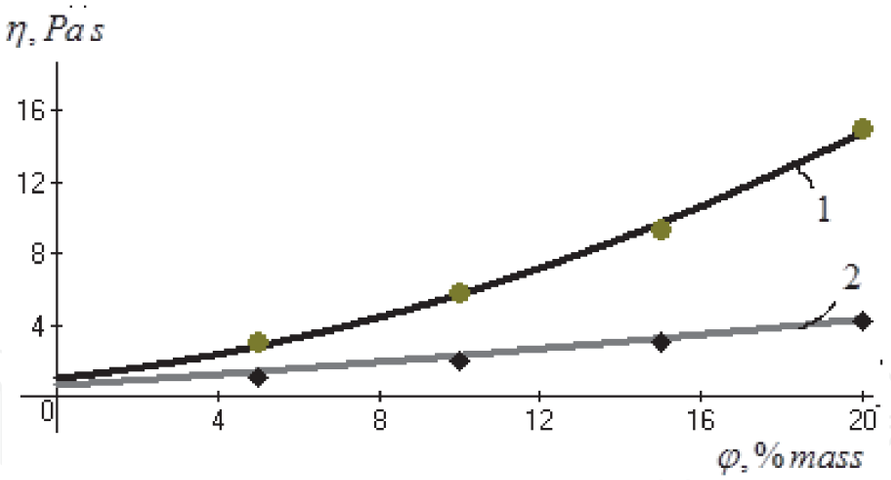

Figure 16.
Dependence of oil viscosity on the content of asphaltenes in it at temperatures: 1–25°C (k_o=0.022); 2–45°C (k_o=0.003).

Figure 15 shows the dependence of the coefficient of consistency on temperature.

The dependence of oil viscosity on the content of asphaltenes (% wt.) in oil using experimental data is expressed by the formula (**Figure 16**)

$$\eta = \eta_0\left(1 + 0.25\varphi + k_0\varphi^2\right) \tag{73}$$

Provided that $\varphi < 10\%$ this expression coincides with the Einstein formula.

In [49], similar studies were conducted for West Siberian oils for the concentration of asphaltenes in oil from 4 to 72% (mass.). This work presents experimental studies of the effective viscosity of non-Newtonian oil as a function of asphaltene content at various temperatures (**Figure 17**). As follows from **Figure 17**, the region of transition from Newtonian to non-Newtonian properties with an increase in the content of asphalt-resinous substances *I* is limited by an abrupt change in the viscosity of oil for all temperatures. Obviously, this is explained by the fact that when the content of asphaltenes is 38–46% (mass.) in West Siberian oil, an abrupt change in the effective viscosity of the oil, structural and mechanical strength, the temperature of the transition to the state of a non-Newtonian fluid, and molecular

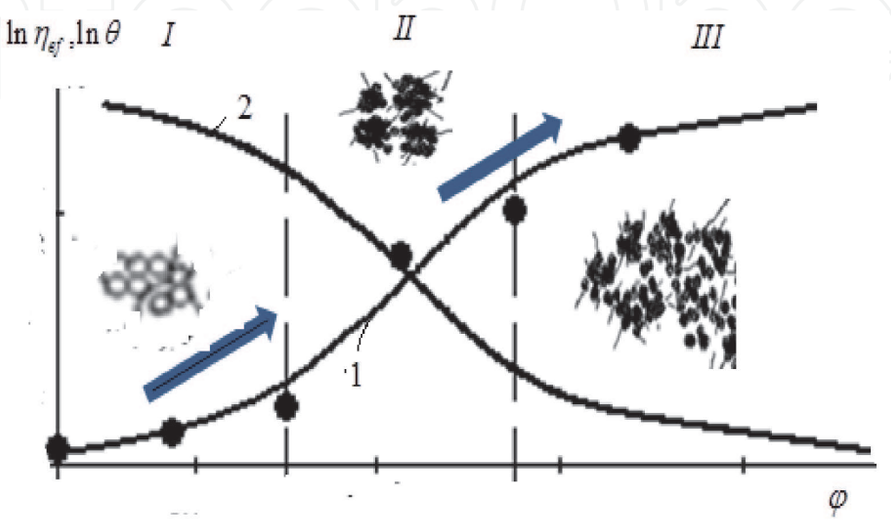

Figure 17.
Characteristic stages of structure formation in oil depending on the content of asphaltenes: I, dispersed oil; II, area of formation of structures; III, structured oil system, 1, viscosity; 2, fluidity.

weight occurs, which is due to the formation of coagulation structures, aggregates, up to the frame throughout the volume. A spasmodic change in viscosity during the period of structure formation (**Figure 17**) and destruction of the structure (**Figure 11**) is a characteristic feature of non-Newtonian oils, which complicates the character of the description of the entire viscosity and mobility curve of the oil system. The process of formation of coagulation structures is associated with an increase in the probability of interaction and collision of particles with an increase in their concentration in the volume. In the next section, problems of coagulation, coalescence of drops and bubbles, and many issues related to solving this problem will be described in detail.

As follows from **Figure 17**, as the structure formation and the concentration of asphaltenes increase, the mobility or fluidity of the oil system decreases, and the fluidity of the system is defined as

$$\ln \theta = \frac{\ln \eta_{\infty}}{\ln \eta_{ef}} \tag{74}$$

Figure 18 shows the experimental data on the change in viscosity of West Siberian oil depending on the asphaltene content [4].

The equation describing the experimental data on the viscosity of oil in large intervals of changes in the content of asphaltenes is presented in the form

$$\ln \mu_{ef} = \ln \eta_0 + b_0 \varphi + b_1 \delta(\varphi) + b_2 \left(1 - \exp\left(-b_3 \varphi^6\right)\right) \tag{75}$$

Here φ is the mass fraction of asphaltenes in oil; b_0–b_3 are the coefficients determined experimentally and depending on temperature; b_1 is the maximum value of the delta function; $\delta(\varphi)$ is the delta function, defined as

$$\delta(\varphi) = \frac{1}{\exp\left(72.5(\varphi - 0.45)\right) + \exp\left(-72.5(\varphi - 0.45)\right)} \tag{76}$$

and η_0 is the initial viscosity,

$$\eta_0 = 2.05x10^{-8} \exp\left(\frac{6075}{T + 273}\right) \tag{77}$$

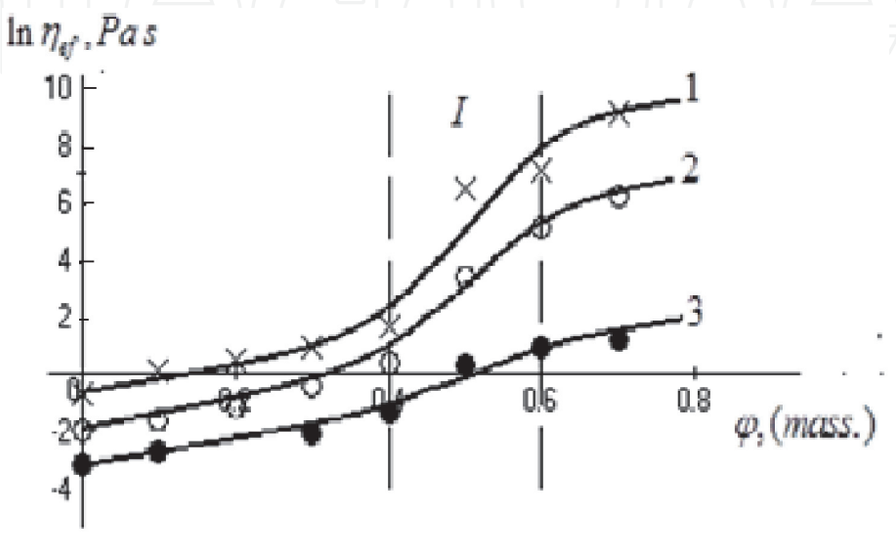

Figure 18.
The dependence of the effective viscosity on the content of the dispersed phase of tar-asphaltene at temperatures: 1–84°C; 2–112°C; 3–144°C. (I—Region of spasmodic structure formation).

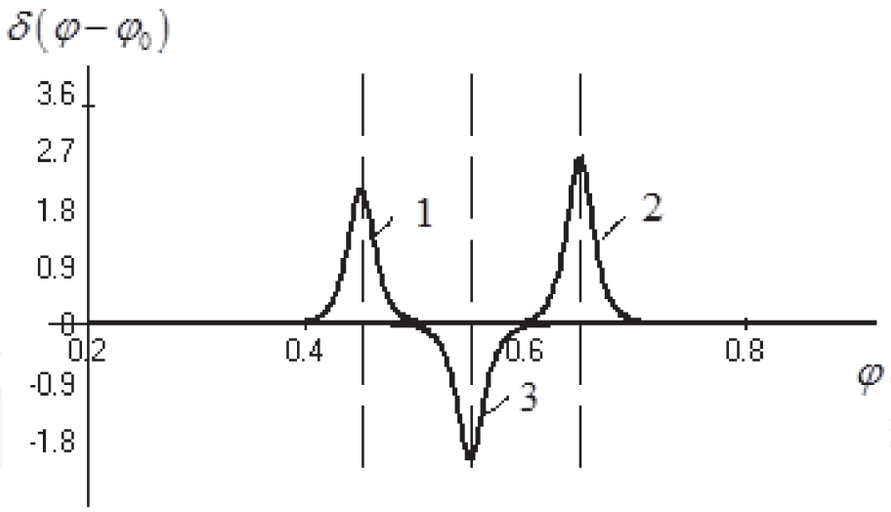

Figure 19.
Delta functions: 1 and 2, positive values of the function $\delta(\varphi) > 0$ *with centers* $\varphi = 0.45, 0.65$*; 3, negative values of the function* $\delta(\varphi) < 0$ *with center* $\varphi = 0.55$.

The value of the delta function characterizes the viscosity jump in the region of structure formation. In particular, the main property of the delta function is as follows

$$\delta(\varphi\text{-}\varphi_0) = \left\{ \begin{array}{ll} 0, & \varphi \neq \varphi_0 \\ \infty, & \varphi = \varphi_0 \end{array} \right\} \tag{78}$$

The expression of the partial approximation of the delta function can be represented

$$\delta(\varphi) = \frac{1}{\exp\left(b_1(\varphi\text{-}\varphi_0)\right) + \exp\left(-b_2(\varphi\text{-}\varphi_0)\right)} \tag{79}$$

Here b_1 and b_2 are the coefficients that determine the width of the base of the delta function, and φ_0 is the coordinate of the center of the jump. **Figure 19** shows various types of delta functions.

Thus, the use of the delta function allows one to describe all the spasmodic phenomena occurring during the formation and destruction of structures in non-Newtonian oil. At the same time, satisfactory results are obtained by using an exponential function of a higher order, which allows one to obtain a smoothing effect in the region of the jump.

The use of aromatic and other solvents partially dissolves asphaltenes, thereby reducing or eliminating the formation of coagulation structures, which improves the rheological properties of dispersed petroleum media. As follows from **Figure 18**, for a given oil, if the asphaltene content is less, the formation of coagulation structures is excluded, although there may be other conditions for different oil fields. An analysis of various studies on the influence of asphalt-resinous substances on the rheology of non-Newtonian oil of various fields leads to conflicting results, although in all cases there is an increase in viscosity as a result of structure formation. It should be noted that in addition to asphaltenes, the rheological properties of the oil disperse system are affected by the content of water and solid phase in it.

4. Evolution of the droplet distribution function in an oil emulsion

Coalescence and fragmentation of droplets significantly change the dispersion of oil emulsions, which is characterized by the evolution of the probability distribution

function over time and size, described by the Boltzmann kinetic equation and the stochastic Fokker-Planck Equation [7, 8, 49, 50]. Changing the size and shape of water droplets in an oil emulsion as a result of their coalescence, deformation, and crushing significantly affects the rheological parameters, in particular, the effective viscosity of the emulsion. Coalescence and crushing of water droplets in emulsions can occur simultaneously. Then the rate of change in the number and size of particles per unit volume is determined by the rates of their coalescence and crushing

$$\frac{dN}{dt} = U_k - U_d \tag{80}$$

where N is the current number of drops in the volume and U_k and U_d are the rates of coalescence and fragmentation of the drops. At a fast droplet crushing rate, the particle distribution function is asymmetric with respect to the maximum and is characterized by a single maximum independent of shear rate, although with slow coagulation, the particle size distribution function can have several maxima and minima, i.e., be multimodal. Moreover, each maximum will characterize the primary, secondary, etc. coagulation of particles of a dispersed medium.

During slow coagulation of solid particles, it is important to construct the evolution of the distribution function over the residence time and size, which gives a complete picture of the change in the number and size of particles over time. In [1, 2], the Fokker-Plank equation is used to construct the evolution of the particle distribution function. The stochastic Fokker-Planck equation describes disperse systems with a continuous change in the properties of the medium and the size of dispersed inclusions. Although the processes of coalescence and fragmentation are characterized by an abrupt change in the properties of particles (sizes), in principle, for a sufficiently long period of time, a change in the average properties can be assumed to be quasicontinuous with an infinitely small jump. In particular, it can be assumed that the average size of droplets and bubbles varies continuously over time and obeys the equation of the change in the average particle mass over time:

$$\frac{dm}{dt} = \omega(a)m \tag{81}$$

Many experimental studies on the fragmentation and coagulation of particles in a turbulent flow show that the average particle size is set at the minimum or maximum level, which corresponds to the aggregative stability of a dispersed medium. Given the above, in Eq. (81) should be considered as the reduced mass relative to the extreme values of the particles, i.e., $m = \frac{\pi}{6}\rho_d(a\text{-}a_{min})^3$ for crushing and $m = \frac{\pi}{6}\rho_d(a\text{-}a_{max})^3$ for coalescence. In particular, based on Eq. (81), we obtain the expression for changing the size of the droplets when they are crushed in the form

$$\begin{aligned} &\frac{da}{dt} = -K(\omega, a)(a\text{-}a_{min}) = m_0 - m_1 a = f(a), m_0 = Ka_{min}, \\ &m_1 = K, t = 0, a = a_0 \end{aligned} \tag{82}$$

being a time-continuous process where $K(\omega, a) = \omega(a)/3 \approx \frac{C_1}{3}\varphi\left(\frac{k_0\dot{\gamma}^{n-1}}{a^2}\right)^{1/3}$ for a power non-Newtonian fluid and $K(\omega, a) = \frac{C_1}{3}\varphi\dot{\gamma}$ for a visco-plastic fluid.

Thus, considering the change in particle size as a continuous function, the Fokker-Planck equation in the simplest case, taking into account (82), can be written as [8, 49, 50].

$$\frac{\partial P(\mathrm{a},\mathrm{t})}{\partial t} = \frac{\partial y}{\partial \mathrm{a}}[P(\mathrm{a},\mathrm{t})(m_0 - m_1 a)] + \frac{B}{2}\frac{\partial^2 P(\mathrm{a},\mathrm{t})}{\partial a^2} \tag{83}$$
$$t = 0, P(\mathrm{a},0) = P_0(\mathrm{a}); a \to 0, P(\mathrm{a},\mathrm{t}) \to 0$$

where B is the coefficient of stochastic diffusion.

The solution to this equation presents great difficulties associated with specifying the form of the function $f(a)$, although some particular analytical solutions of Eq. (83) depending on the nature of the function can be found in [8, 49, 50].

The solution of Eq. (83) by the method of separation of variables will be presented in the form

$$P(r,t) = r^{\theta}\exp\left(\frac{ka_0^2 r^2}{2B}\right)\sum_{n=0}^{\infty} C_n L_n^{(\alpha)}\left(\frac{ka_0^2 r^2}{2B}\right)\exp(-2knt) \tag{84}$$

where $\theta = {}^{m_R a_0^2}\!/_{B}$, $\alpha = \frac{m_R a_0^2 - B}{2B}$, $L_n^{(\alpha)}$ Laguerre functions, and

$$C_n = \frac{\theta^{\frac{\theta+1}{2}}\int_0^{\infty} P_0(r) L_n^{(\alpha)}\left(\frac{ka_0^2 r^2}{2B}\right)dr}{2^{\frac{\theta-1}{2}}\Gamma\left(n+\frac{\theta+1}{2}\right)m^{\frac{\theta+1}{\theta}}n!} \tag{85}$$

Solutions (84) and (85) characterize the evolution of the probability density distribution function of droplets in size and in time. The asymptotic value of the distribution for i $t \to \infty$ s is obtained from solution (84), taking into account the properties of the Laguerre function, in the form

$$P_{\infty}(r) = C_R r^{\theta}\exp\left(-\frac{ka_0^2 r^2}{2B}\right) = C_{PR} a^{\theta}\exp\left(-ba^2\right) \tag{86}$$

$$C_{PR} = 2a_0^{-\theta}\left(\frac{\theta}{2m}\right)^{\frac{\theta+1}{2}}, \quad b = {}^{k}\!/_{2B}$$

Having introduced some simplifications taking into account the initial distribution in the form of a lognormal function $P_0(a) = A_0(a)\exp\left(-m_0(\ln a - \alpha_0)^2\right)$ and the limiting distribution (86) taking into account the experimental data for the family of distribution curves with a number m, with some assumptions in a more simplified form, we obtain

$$P(a,t) = \sum_{n=0}^{\infty} A_n(t)\exp\left[-m_n(t)(\ln a - \alpha_{sn})^2\right] \tag{87}$$

where $\alpha_{sn} = \ln a_s$ is the parameter corresponding to the logarithm of the maximum value of each extremum.

Figure 20 shows the evolution of the distribution function of the fragmentation of a non-Newtonian viscoelastic drop (oil) in an aqueous medium.

The spectrum of large and small droplets is practically shifted relatively to each other [8, 49] (**Figure 20**).

It is important to note that the fluctuation of the distribution function on the left side of the curve indicates secondary, tertiary, etc. the nature of droplet crushing, and on the right side - about their multiple coalescence. However, after some time, when the resources of the large-droplet or small-droplet spectrum are exhausted,

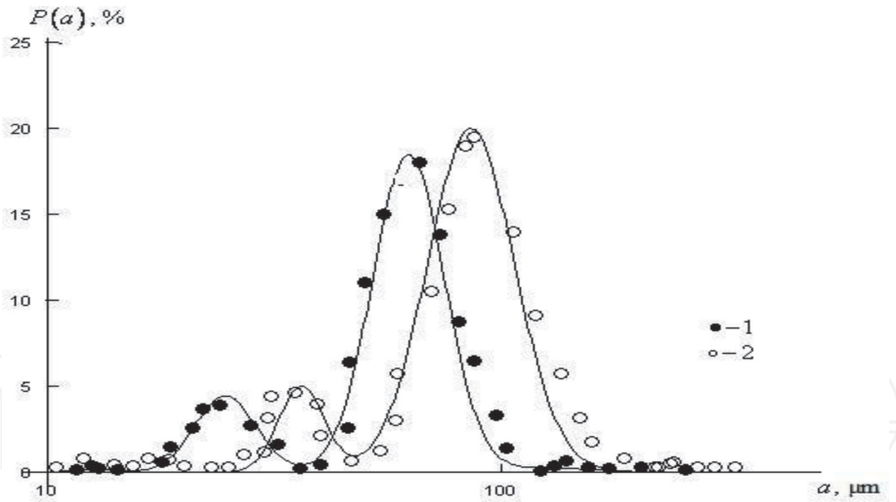

Figure 20.
The characteristic distribution of the distribution function during crushing drops in size and time equal to 1, 10 min., and 2, 20 minutes.

the spectrum begins to behave like a single-humped one. In practice, the behavior of multi-hump distributions in the model representation is confirmed when the distribution is represented by the sum of two or more distribution functions. The character of the evolution of the distribution function and the change in the coefficient of turbulent diffusion can also be significantly affected by the deposition of particles from the turbulent flow. The distribution spectrum varies significantly with a change in the droplet deposition rate. In conclusion, we note that the phenomena of coalescence and fragmentation of droplets are spasmodic. In the case of small jumps, such processes are satisfactorily described by the Fokker-Planck equation. Obviously, jumps should become smaller and more likely, so the diffusion process can always be approximated by a jump process, but not vice versa.

5. Discussion of results and conclusions

The content in the composition of crude oil of various particles of the dispersed phase significantly affects the rheological parameters of the liquid. The main phenomena in the processes of coalescence of water droplets in oil emulsions are the destruction of the adsorption film on the surface due to asphalt-resinous substances, the thinning and rupture of the interfacial film between the droplets, and the coalescence of droplets.

The formation and formation of the adsorption layer is described by Eq. (5), a comparison of which with experimental data gives satisfactory results. The equation for estimating the thickness of the adsorption layer is given in (4). To study the thinning of the interfacial film, Eqs. (17) and (18) are derived that take into account the presence of dynamic, capillary, proppant pressure and the Marangoni effect. Particular cases of solving proposed Eqs. (20)–(24) are presented. Comparison with the experimental data on the thinning of the interfacial film [38] for West Siberian oils (**Figure 5**) showed that for large values of the film thickness, Eq. (20) with coefficients equal to $b_3 = 1.2.10^{-3}$ is the most suitable, and coefficient β_1 is shown in **Table 3**.

For very thin films $\delta \leq \delta_{kp}$, expression (21) with a coefficient $b_3 = 0.098$ is suitable, and the change in surface tension is described by the formula $\sigma = (3.6 + (\sigma_0 - 3.6)\exp(-23.1C)) \times 10^{-3}, H/м.$

C,g/l	0,10	0,20	1,00	1,20
β_1	0.14	0.235	0.265	0.30

Table 3.
The dependence of the coefficient β_1 on the concentration demulsifier.

After reaching the critical value of the thickness $\delta \leq \delta_{кр}$, spontaneous thinning and interfacial film breaking occur (**Figure 5**). As follows from formulas (17)–(23), a proppant pressure, inversely proportional to the film thickness and depending on the asphaltene content in oil and the concentration of demulsifier, plays an important role in thinning and rupture of an interfacial film.

The presence of two-dimensional pressures and the complexity of its distribution on the film surface, taking into account Eq. (14), show that, when it is thinned, the presence of the Marangoni effect to some extent helps to stabilize oil emulsions, i.e., has an inhibitory effect on tearing the film. As follows from Eq. (20) and the formula for determining the coefficient, the Marangoni effect contributes to the temporary stabilization of the interfacial film, since at any point where the film becomes thinner due to the influence of external forces, a local increase in surface tension occurs, which counteracts the thinning. The process of thinning and rupture of the film is random (spontaneous) in nature, and the probability of its rupture is inversely proportional to its thickness.

The main physical phenomena that occur in oil emulsions are the coalescence of droplets in the presence of asphalt-resinous substances in the oil, leading to structure formation. An analytical solution of the equation of diffusion transfer of droplets in an isotropic turbulent flow determines the coalescence and fragmentation frequencies of droplets (29–31).

The paper proposes many expressions for determining the structural viscosity of oil from the content of water droplets, as well as the empirical or semiempirical dependences of the oil viscosity on the content of asphalt-resinous substances (73) for Iranian oil and (81) for West Siberian oil. Theoretical and experimental studies have shown that the value of the structural viscosity of oil during structure formation sharply increases, and when the structure is destroyed, it sharply decreases (**Figure 11**).

Based on the Fokker-Planck equation, the evolution of the distribution function of water droplets in an oil emulsion as a function of size and time is studied (84) and (85).

The intensification of the processes of flow and separation of oil emulsions is associated primarily with the rheological properties of the oil emulsion and turbulization of the flow. High-frequency turbulent pulsations contribute to the mechanical weakening of the adsorption and interfacial film and intermolecular bonds between its components, a decrease in the strength and destruction of the film as a result of their deformation (tension, compression), and improvement of the conditions of mutual effective collision (increase in the collision frequency) and coalescence.

Acknowledgements

This work was supported by the Science Foundation of «SOCAR» under the grant project 04LR - AMEA (10/09/2019) at the Institute of Catalysis and Inorganic Chemistry named after Acad. M.F.Nagiyev.

Nomenclature

A	van der Waals-Hamaker constant;
b_1, b_2, b_3	coefficients in Eq. (18)
a	diameter of drops
C	concentration
c_P	heat capacity
D	molecular diffusion coefficient
D_T	droplet diffusion coefficient
d	pipe diameter
f	resistance coefficient in pipes
F	the force acting on the interfacial film
F_g	hypergeometric function
H	height of the intermediate layer
g	acceleration of gravity
I	mass flow to the surface of a drop per unit time
$P(a,t)$	size distribution function of the probability of droplets
R_K	interfacial film radius
R	drop radius
P	pressure
T	temperature
V_P	particle velocity
V	flow rate in the film
U	flow rate
$\overline{U}^2$	mean square velocity
t	time
Γ	the concentration of adsorbed matter
δ	film thickness
$\dot{\gamma}$	shear rate
δ_0	initial film thickness
Δ	the thickness of the adsorbed layer
ε	the porosity of the intermediate layer
ε_R	specific energy dissipation
ν_C	kinematic viscosity of the medium
η	film viscosity
η_c	dynamic viscosity of the medium
η_d	dynamic viscosity of a drop
η_{ef}	effective viscosity of emulsions
λ	coefficient of thermal conductivity
μ_P	the degree of entrainment of drops by a pulsating medium
μ	eigenvalues
σ	surface tension
Π	proppant pressure
ρ_C	medium density
ρ_d	droplet density
τ_P	relaxation time
τ	shear stress
φ	volume fraction of droplets in the stream
ω	collision frequency
$\mathrm{Mo} = \frac{g\eta_c^4}{\rho_c\sigma^3}\frac{\Delta\rho}{\rho_c}$	Morton's number
$\mathrm{Pe} = \frac{Ua_r}{D}$	Peclet number

$\mathrm{Re} = \frac{V_p d}{\nu_c}$	Reynolds number
$\mathrm{We} = \frac{\rho_c U^2 a}{\sigma}$	the Weber number

Indices:

0	initial conditions
p	particle
c	medium

Author details

Gudret Isfandiyar Kelbaliyev, Dilgam Babir Tagiyev and Manaf Rizvan Manafov*
Azerbaijan National Academy of Sciences, Nagiyev Institute of Catalysis and Inorganic Chemistry, Baku, Azerbaijan

*Address all correspondence to: mmanafov@gmail.com

References

[1] Lissant L. Emulsion and Emulsion Technology. New York: Marsel Dekker; 1976. p. 211

[2] Sjoblom J, Urdahl O, Hoiland H, Christy AA, Johansen EJ. Water in crude oil emulsions formation, characterization and destabilization. Progress in Colloid and Polymer Science. 1990;**82**:131

[3] Pozdnyshev GN. Stabilization and Destruction of Oil Emulsions. Moscow: Nedra; 1982

[4] Tronov VP. The Destruction of Emulsions in Oil Production. Moscow: Nedra; 1974. p. 314

[5] Tirmizi NP, Raghurankan B, Wiencek J. Demulsification of water/oil/solid emulsions by hollow-fiber membranes. AICHE Journal. 2004; **42**(5):1263

[6] Danae D, Lee CH, Fane AG, Fell CJD. A fundamental study of the ultrafiltration of oil-water emulsions. Journal of Membrane Science. 1987;**36**: 161

[7] Kelbaliev GI, Rasulov SR. Hydrodynamics and Mass Transfer in Dispersed Media. ChemIzdat: St. Petersburg; 2014. p. 567

[8] Kelbaliyev GI, Tagiyev LB, Rasulov SR. Transport Phenomena in Dispersed Media. Boca Raton, London, New York: Taylor and Francis Group, CRC Press; 2019. p. 424

[9] Sarimeseli A, Kelbaliyev G. Modeling of the break-up of deformable particles in developed turbulent flow. Chemical Engineering Science. 2004;**59**(6): 1233-1240

[10] Kelbaliyev G, Sarimeseli A. Modeling of drop coalescence in isotropic turbulent flow. Journal of Dispersion Science and Technology. 2006;**27**:443

[11] Migashitani K, Yamauchi K, Mastuno Y. Coalescence of drop in viscous fluid. Journal of Chemical Engineering. 1985;**18**:299

[12] Colaloglou CA, Tavlarides II. Description of interaction process in agitated liquid-liquid dispersions. Chemical Engineering Science. 1977;**32**: 1289

[13] Soo SL. Fluid Dynamics of Multiphase Systems. London: Blaisdell Puiblishing; 1970

[14] Hirschberg A, DeJong NL, Schipper BA, Meijer JG. Influence of temperature and pressure on Asphaltene flocculation. Society of Petroleum Engineers. 1984;**24**(3):283

[15] Laux H, Rahiman I, Browarzik D. Flocculation of asphaltenes at high pressure. I. Experimental determination of the onset of flocculation. Petroleum Science and Technology. 2001;**19**(9/10): 1155

[16] Mulhins OC, Shey EY. Structures and Dynamics of Asphaltenes. New York: Plenum Press; 1998

[17] McLean J, Kilpatrick PK. Effects of asphaltene solvency on stability of water crude oil emulsions. Journal of Colloid and Interface Science. 1997;**189**(2):242

[18] Levich VG. Physicochemical Hydrodynamics. Moscow: Fizmatgiz; 1962

[19] Ermakov SA, Mordvinov AA. On the effect of asphaltenes on the stability of oil-water emulsions. Oil and Gas Business. 2007;**10**:1

[20] Wegener M, Fevre M, Wang Z, Paschedag A, Kraune M. Marangoni convection in single drop flow – Experimental investigation and 3D-simulation. In: 6th International Conference of Multiphase Flow. Leipzig, Germany; 2007. p. 9

[21] Fanton X, Cazabat AM, Quyru D. Thickness and shape of films driven by a Marangoni flow. Langmuir. 1996;**12**: 5875

[22] Leo LY, Matar OK, Perez de Ortir ES, Hewitt GF. A description of phase inversion behavior in agitated liquid-liquid dispersions under the of Marangoni effect. Chemical Engineering Science. 2002;**57**:3505

[23] Scheludko A. Thin liquid film. Advances in Colloid and Interface Science. 1967;**11**:391

[24] Chen JD, Slattery JC. Effects of London-van der Waals forces on the thinning of a dimpled liquid films as a small drop or bubble approaches a horizontal solid phase. AICHE Journal. 1990;**28**(6):955

[25] Petrov AA, Blatov SA. Study of the stability of hydrocarbon layers at the interface with aqueous solutions of demulsifiers. Chemistry and Technology of Fuels and Oils. 1969;**5**: 25-33

[26] Liao Y, Lucas D. A literature review of theoretical models for drop and bubble breakup in turbulent dispersions. Chemical Engineering Science. 2009;**64**(15):3389-3395

[27] Altunbas A, Kelbaliyev G, Ceylan K. Eddy diffusivity of particles in turbulent flow in rough channels. Journal of Aerosol Science. 2002;**33**:1075

[28] Wang T, Wang J, Jin Y. A novel theoretical breakup kernel function for bubbles/droplets in a turbulent flow. Chemical Engineering Science. 2003;**58**: 4629-4636

[29] Chatzi E. Analysis of interactions for liquid–liquid dispersions in agitated vessels. Industrial and Engineering Chemistry Research. 1987;**26**:2263-2272

[30] Chatzi E, Kiparissides C. Dynamic simulation of bimodal drop size distributions in low-coalescence batch dispersion systems. Chemical Engineering Science. 1992;**47**:445-456

[31] Alopaeus V. Simulation of the population balances for liquid–liquid systems in a nonideal stirred tank. Part 2: Parameter fitting and the use of the multiblock model for dense dispersions. Chemical Engineering Science. 2002;**57**: 1815-1826

[32] Lehr F, Milles M, Mewes D. Bubble-size distributions and flow fields in bubble columns. AICHE Journal. 2002; **48**:2426-2436

[33] Raymond F, Rozant JM. A numerical and experimental study of the terminal velocity and shape of bubbles in viscous fluids. Chemical Engineering Science. 2000;**57**:943-953

[34] Liu L, Yan H, Zhao G. Experimental studies on the shape and motion of air bubbles in viscous liquids. Experimental Thermal and Fluid Science. 2015;**62**: 109-121

[35] Batchelor GK. The effect of Brownian motion on the bulk stress in a suspension of spherical particles. Journal of Fluid Mechanics. 1977;**83**:97-117

[36] Krieger IM, Dougherty TJ. A mechanism for non-Newtonian flow in suspensions of rigid spheres. Transactions. Society of Rheology. 1959; **N3**:137-152

[37] Quemada D. Rheology of concentrated disperse systems and

minimum energy dissipation principle I. Viscosity-concentration relationship. Rheologica Acta. 1977;**16**:82-94

[38] Brownstein BI, Schegolev VV. Hydrodynamics, mass – and heat transfer in column apparatus. Moscow: Chemistry; 1988. 325p

[39] Khodakov GS. Rheology of suspensions. The theory of phase flow and its experimental justification. Ross Khim Zh. 2003;**XLVII**(2):33-41

[40] Vielma JC. Rheologocal Behavior of Oil-Water Dispersion flow in horizontal pipes. A thesis submitted in partial fulfillment of the requirements for the degree of Master of Science in the Discipline of Petroleum Engineering. The University of Tulsa; 2006

[41] Mewis J, Wagner NJ. Colloidal Suspension Rheology. Cambridge, UK: Cambridge University Press; 2012

[42] Kelbaliyev GI, Rasulov SR, Mustafayeva GR. Viscosity of structured disperse systems. Theoretical Foundations of Chemical Engineering. 2018;**52**(3):404-411

[43] Oil Emulsions. Available from: http://petrowiki.org/Oil emulsions

[44] Kroy K, Capron I, Djabourov M, Thermique P. ESPCI. Paris. France; 1999

[45] Krassimir D. Danov on the viscosity of dilute emulsions. Journal of Colloid and Interface Science. 2001;**235**:144-149

[46] Argillier JF, Coustet C, Hénaut I. Heavy oil rheology as a function of asphaltene and resin content and temperature. SPE/Petroleum Society of CIM/CHOA 79496, International Thermal Operations and Heavy Oil Symposuim and International Horizontal Well Technology Conference. 2002

[47] Davarpanah L, Vahabzadeh F, Dermanaki A. Structural study of Asphaltenes from Iranian heavy crude oil. Oil and Gas Science and Technology. 2015;**70**(6):1035-1049

[48] Mukhmedzyanova AA, Buduik VA, Alyabev AS, Khaybullin AA. Influence of temperature and asphaltenes concentration on rheological properties of disperse systems of the west Siberian oils tar. Bashkir Chemical Journal. 2012; **19**(4):1-4

[49] Sis H, Kelbaliyev G, Chander S. Kinetics of drop breakage in stirred vessels under turbulent conditions. Journal of Dispersion Science and Technology. 2005;**26**:565

[50] Gardiner CW. In: Haken H, editor. Handbook of Stochastic Methods for Physics, Chemistry and the Natural Sciences. New York: Springer; 1985